UNIVERSIDADE DO ALGARVE

NOTABLE DIFFERENCES IN GENE EXPRESSION BETWEEN INJURED TURBOT (Scophthalmus maximus) AND BRILL (Scophthalmus rhombus) SKIN

João Luis Correia Estêvão

Dissertação

Mestrado Integrado em Engenharia Biológica

Trabalho efectuado sob a orientação de

Professor Doutor Paulino Martinez Portela

Professora Doutora Deborah Mary Power

2015

UNIVERSIDADE DO ALGARVE

NOTABLE DIFFERENCES IN GENE EXPRESSION BETWEEN INJURED TURBOT (Scophthalmus maximus) AND BRILL (Scophthalmus rhombus) SKIN

João Luis Correia Estêvão

Dissertação

Mestrado Integrado em Engenharia Biológica

Trabalho efectuado sob a orientação de

Professor Doutor Paulino Martinez Portela

Professora Doutora Deborah Mary Power

2015

Dedicado ao meu avô, à minha mãe e à minha irmã

AGRADECIMENTOS

Esta tese de mestrado é fruto de trabalho em equipa de um ano. Porém, todo o meu conhecimento e trabalho elaborado provem de um esforço e caminho feito ao longo de seis anos. Várias pessoas contribuíram para que esta meta fosse atingida mas, principalmente, as que participaram nesta fase final foram, sem dúvida, as mais marcantes e importantes.

Quero, primeiro, agradecer às pessoas que me apoiaram ao longo destes seis anos pela compreensão, paciência e suporte incondicional que me deram durante toda esta fase. Portanto, quero agradecer aos meus amigos de sempre, nomeadamente ao Tiago Maria, ao Jerome Martins, ao Ricardo Rodrigues, ao Luís Gomes e ao Fábio Bravo. Sem eles, provavelmente, não teria chegado até aqui.

Quero também agradecer a quem me apoiou já nesta fase final do mestrado que, para mim, têm tanto significado na minha vida como os meus amigos de sempre. Quero agradecer ao Jorge Pontes, à Vanda Baltazar, à Marta Gonçalves, à Sandra Maceiras e à Laura Silva pelo apoio antes e durante esta etapa final do meu curso. Foram também como uma família para mim.

Outras pessoas às quais queria agradecer e que são ainda mais marcantes são a toda a família Pinheiro do Porto, que sempre tão bem me têm acolhido que me considero um integrante da família. A eles, um enorme obrigado por sempre me receberem de braços abertos.

Outro agradecimento muito grande e especial é a uma pessoa que, para além de grande amiga, é como uma irmã para mim. Quero agradecer especialmente à Elena Pimentel por sempre me ter apoiado durante a minha estadia inicial fora do meu país e me orientado e compreendido em todas as minhas fases da minha estadia. Ainda hoje continua apoiando-me incondicionalmente e sempre lhe estarei grato por sempre me dar esperança e força nas fases mais complicadas, mas também por grandes momentos de amizade e em família partilhados.

Quero agradecer a toda a equipa dos departamentos de Genética e de Anatomia Patológica da Faculdade de Veterinária de Lugo por me terem aceitado, apoiado, ajudado e nunca terem perdido a confiança em mim. Foi um enorme prazer e sorte poder ter trabalhado com todos pois, para além de excelentes profissionais, são como uma família unida fazendo sentir-me como se estivesse em casa.

Quase finalizando, quero dar o meu eterno agradecimento aos professores Deborah Power e Paulino Martinez por sempre terem acreditado e confiado em mim e nas minhas capacidades, embora existisse momentos em que não acreditasse que as tinha. À professora Deborah Power agradeço imenso o facto de me ter aberto as portas para o futuro, confiando-me este bonito projeto e de não ter desistido de mim. Ao professor Paulino Martinez os agradecimentos são eternos, pois apoiou-me, ajudou-me durante todo o projeto, orientou-me da melhor maneira possível, teve uma enorme paciência, camaradagem e capacidade de trabalho. Sinto que um dia gostaria de ter estas grandes qualidades profissionais e humanas que estas enormes pessoas têm.

Por fim, quero agradecer ao pilar da minha chegada a esta meta, que é a minha família. Portanto, quero agradecer ao meu avô, José de Brito Correia, à minha mãe, Ana Maria Valentim Correia Estêvão e à minha irmã, Ana Luisa Correia Estêvão Rodrigues, por todo o apoio financeiro, emocional e pela educação e experiência de vida que sempre partilham comigo e que faz de mim hoje o homem que sou. A eles devo tudo o que tenho hoje.

ABSTRACT

The skin, the largest organ of fish's body and first barrier against external agents, plays a crucial role against environmental aggressions and is decisive in communication between individuals. Cutaneous lesions are common in fish and may result in an open door for infectious agents and originate osmotic stress, which can be life threatening for the animal. Turbot (*Scophthalmus maximus*) and brill (*Scophthalmus rhombus*) are two closely related congeneric species with striking differences in their skin, since turbot presents tubercles instead of the scales found in brill. In this work, gene expression analyses were performed in order to analyze the genetic differences in the skin response between the two species. Skin scraping areas (72 h after injury) from three biological replicates of each species were compared with normal skin areas from the same individuals. A previously reported 4x44k Agilent turbot microarray was employed, after evaluating its suitability by comparison of the base sequence of common genes using bioinformatics. Skin-related genes from previous studies (1564 sequences) were taken as a reference to screen the turbot database and the oligo-probes in the microarray. Among them, 584 (~37%) were present in the turbot database (e-value < $9x10^{-20}$) and 326 (~21%) contained oligo-probe in the microarray, a notable result since the microarray was especially enriched with immune-related organs. Genes with a significant fluorescent signal in the microarray (>200 fluorescence units) were identified in each (turbot: 15,739; brill: 12,393) and in both species (10,065). Among them, 1750 differentially expressed genes (t-test p-value $p<0.005$; $\log_2$ ratio <-2 and >2) were detected in brill, 1461 in turbot, and 885 showed differences between species, respectively. These results strongly suggest: 1) the turbot microarray is suitable for gene expression analysis in brill, and 2) a notable different occurs in the response of the skin to damage in the two species.

Keywords: Brill, gene expression, innate immunity, oligo-microarray, skin, turbot

RESUMO

A pele dos vertebrados tem um papel crucial na separação do "interior" do indivíduo do "exterior", funcionando como uma interface para comunicação e contacto. Esta funciona tanto como barreira contra agentes microbiológicos, físicos e químicos/bioquímicos, bem como um órgão complexo que desempenha funções essenciais em conjunto com os seus apêndices, tais como, termorregulação, síntese hormonal, funções sensoriais, metabolismo, homeostasia osmótica, comunicação entre indivíduos, elaboração de estruturas especiais e produção de várias substâncias específicas. Lesões cutâneas e doenças associadas são mais frequentes em peixes do que em vertebrados terrestres e correspondem a um dos fatores primários que condicionam a estrutura da sua pele. Estas, para além de serem, geralmente, pouco específicas e indicativas de uma doença local ou da manifestação de uma doença sistémica, podem originar *stress* osmótico e representam uma entrada a agentes infeciosos que pode ser ameaçador à saúde destes seres-vivos.

A pele dos peixes, tal como em vertebrados, é composta por três camadas principais: Epiderme, derme e hipoderme. Para além disso, estas camadas dividem-se em vários estratos sendo, em teleósteos, a epiderme composta por cutícula e membrana basal; a derme composta por estrato esponjoso e estrato compacto; e a hipoderme correspondente à tela subcutânea. A epiderme funciona, portanto, como a primeira barreira molecular do sistema imunitário. As escamas são o componente primário do esqueleto da derme em peixes e em teleósteos apresentam-se como placas flexíveis calcificadas incluídas parcialmente entre as bolsas das escamas e orientadas posteriormente (escamas elasmoides). Para além disso, as escamas representam uma reserva de fonte de cálcio que pode ser utilizada em períodos de fome ou de pré-desova, por exemplo. A derme fornece ainda uma integridade estrutural e força de tensão ao integumento, resultando numa rigidez à flexão e maior eficiência à excursão do esqueleto e, assim, numa locomoção mais eficiente. Por outro lado, a hipoderme é menos desenvolvida em peixes, funcionando como uma reserva de energia, uma barreira à difusão de fluidos e como um amortecedor dos choques.

A resolução das lesões cutâneas é altamente dependente da temperatura. Contudo, a cobertura e regeneração epidérmica, em peixes, é menos afetada pela temperatura, sendo a epitelização terminada entre as 6 e 8 horas após a lesão. Depois disso, o processo lento de reconstituição epitelial toma lugar e, por fim, a reconstituição da derme. As lesões

cutâneas têm, portanto, um tempo de regeneração da pele de aproximadamente 35 dias. A regeneração das escamas acontece de um modo similar ao da sua ontogénese e tem começo após o encerramento da lesão. Estas desenvolvem-se dentro das bolsas das escamas e têm um crescimento geralmente contínuo, com algumas influências e restrições causadas por fatores intrínsecos e extrínsecos, tais como, períodos de pouca atividade e períodos de *stress* e de deficiência de cálcio.

Apesar da grande importância da pele em peixes como barreira imune e como tecido regenerante, pouco se conhece acerca dos genes e processos moleculares envolvidos no processo de resposta imunitária e de regeneração deste tecido.

O rodovalho (*Scophthalmus rhombus* (Linnaeus, 1758)) e o pregado (*Scophthalmus maximus* (Linnaeus, 1758)) são duas espécies congéneres de peixe plano (*Pleuronectiformes*) fortemente relacionadas, tanto relativamente à sua distância genética, bem como ao seu cariótipo e à morfologia e função da pele. No entanto, estas duas espécies apresentam uma notável diferença na sua pele, devido ao facto do rodovalho conter escamas e o pregado conter tubérculos.

Neste trabalho analisou-se as diferenças genéticas ocorrentes durante a resposta da pele a uma perturbação entre as duas espécies, 72h após uma escarificação, tomando uso de um *oligo-microarray* enriquecido com genes relativos à resposta imunitária, previamente desenhado para pregado.

Uma lista inicial de 1564 genes que se expressam em pele de peixe, provenientes de estudos anteriores, foi usada para verificar a presença de genes da pele na base de dados do pregado e no *microarray* e também a sua adequação para a avaliação dos perfis de expressão génica em rodovalho. De entre estes, 584 genes (~37%) estão presentes na base de dados do pregado e 326 (~21%) contém oligonucleótido no *microarray*. Esta é uma notável presença de genes relacionados com a pele no *microarray* e na base de dados.

Doze indivíduos (6 rodovalhos e 6 pregados), mantidos nas suas respetivas condições de cultivo, sofreram uma escarificação na qual a zona mais exterior da pele foi retirada. Em seguida, foram mantidos nas suas respetivas condições de cultivo durante 72h. A esta altura, amostras de pele da zona ferida e da zona normal foram colhidas para análise de expressão génica, bem como amostras de pele e músculo de ambas as zonas para avaliação histológica da qualidade das amostras. Posteriormente, seis indivíduos (3 por espécie) foram escolhidos para a análise de expressão génica após consideração da qualidade das amostras de ARN extraído e de secções de pele, tendo como base de consideração amostras com o melhor número de integridade do ARN, com um dano

moderado na pele (remoção de epiderme e derme superior) e com um menor número de artefactos possível.

Após hibridização das amostras no *microarray* e normalização dos dados, um filtro de intensidade de fluorescência (> 200 unidades de fluorescência) foi aplicado de modo a evitar a presença de valores falsos positivos. Portanto, o número de genes com um sinal de fluorescência consistente foi de 15739 genes expressados em pregado, 12393 genes expressados em rodovalho e 10065 genes expressados em ambas as espécies. Um número considerável de genes expressados em pregado é observável, como seria de esperar. No entanto, observou-se também um número notável de genes expressados em rodovalho que, em conjunto com a notável presença de genes relacionados com a pele evidenciada anteriormente, demonstram uma forte viabilidade do *microarray* na análise dos genes expressados em rodovalho e também a adequação do *microarray* para rodovalho e para genes relacionados com a pele. Para além disso, denotou-se também uma apreciável quantidade de genes partilhados em ambas as espécies, o que corrobora a proximidade genética entre rodovalho e pregado evidenciada em estudos anteriores.

Na identificação dos genes diferencialmente expressados em cada espécie e entre espécies elaborou-se duas listas para cada análise executada, sendo estas baseadas no valor do $\log_2$ razão e no teste t de *student*. Identificaram-se, em resposta à lesão, 1750 genes diferencialmente expressados em rodovalho, 1461 em pregado e 885 genes demonstraram diferenças de expressão entre espécies. Estes resultados sugerem uma maior resposta em rodovalho do que em pregado e uma diferença observável na resposta a uma perturbação na pele entre ambas as espécies. Contudo, salientou-se o facto de o pregado apresentar um maior desvio-padrão entre os valores de expressão génica das réplicas biológicas (indivíduos) do que o rodovalho, o que pode ter sido causado pela diferença estrutural na pele do pregado em relação ao rodovalho e que pode resultar numa análise menos rigorosa para esta espécie.

Os 326 genes referentes à lista inicial de 1564 genes relacionados com a pele e que estão presentes no *microarray* foram usados, em conjunto com genes já identificados em estudos anteriores, para verificar os seus níveis de expressão em cada espécie e quais se diferenciam entre espécies. Para além disso, verificou-se a função putativa dos genes mais diferencialmente expressados em cada espécie e entre espécies e também os termos de Ontologia Génica e metabolismos aos quais estes eram classificados. No total, 7 genes em pregado, 3 em rodovalho e 8 entre espécies não foram associados a qualquer termo de Ontologia Génica. Os resultados observados em pregado demonstraram uma inibição nas

funções de desenvolvimento e organização da pele e do esqueleto e um maior dispêndio em funções relativas à resposta imunitária. Em rodovalho observou-se um dispêndio em funções relativas à regeneração epitelial, enquanto funções relativas a desenvolvimento da musculatura foram inibidas. As funções que se diferenciaram entre as espécies foram regeneração, reparação e organização da pele.

Usaram-se 9 genes para validação dos resultados do *microarray* em pregado e 6 genes para validação em rodovalho, através de um PCR em tempo real. Embora o número de genes utilizados tenha sido pequeno, a alta e significante correspondência observada entre o PCR e o *microarray* sugere a consistência dos resultados obtidos para ambas as espécies.

Este estudo confere a proximidade genética existente entre rodovalho e pregado, mostrando também diferenças genéticas na regeneração da pele, possivelmente relacionadas com a sua diferente estrutura.

Palavras-chave: Pele, rodovalho, pregado, *oligo-microarray*, imunidade inata

INDEX

1. ABREVIATIONS

BLAST	Basic local alignment search tool
Bp	Base pairs
cDNA	Complementary deoxyribonucleic acid
cRNA	Complementary ribonucleic acid
Cy3-CTP	Cyanine 3 - cytidine triphosphate
DAVID	Database for annotation, visualization and **i**ntegrated discovery
DB4	Turbot 4 database
DB5	Turbot 5 database
DE	Differentially expressed
Eda	Ectodysplasin
FGF	Fibroblast growth factor
GO	Gene ontology
H-E	Haematoxylin-eosin
HM	Turbot treatment sample
hs	Brill treatment sample
ID	Identity
LOESS method	Local regression method
MeV	MultiExperiment Viewer
NCBI	National Center for Biotechnology Information
PBS	Phosphate-buffered saline
PCR	Polymerase chain reaction
PFA	Paraformaldehyde
QPCR	Quantitative-polymerase chain reaction
RIN	RNA integrity number
RNA	Ribonucleic acid
RPS4	Ribosomal protein S4
RT-PCR	Real time-polymerase chain reaction
sa	Brill control sample
SM	Turbot control sample
TNF	Tumor necrosis factor

2. INTRODUCTION

Biological Engineering is featured by engineering and biological knowledge which serve for the development of systems, methodologies and processes that take advantage of biological components for specific applications which points to answer for the various society problems (Universidade do Algarve 2013). Animal production and improvements through breeding and husbandry when considered in the context of aquaculture production are part of the current developments in blue biotechnology. The present study that takes a molecular and morphological approach to studying skin repair in teleosts provides the basis for future studies targeting the barrier function of skin and provides essential knowledge that can be used for maintenance of healthy fish and in this way improving production. The next points will give an overview of the basic structure of skin in vertebrates and, specifically, in teleosts. Moreover, it will introduce the skin repair and regeneration theme by giving a histological overview of the general process. An information about the species studied in this work togheter with the actual molecular knowledge about the skin repair and regeneration and the aim of the work is also provided.

2.1. Skin structure

The vertebrate's skin has a crucial function in separating the individual's 'inside' from its environment working as an interface for communication and contact with the 'outside'. As a barrier, it protects from microbiological, physical and chemical/biochemical agents (Figure 2.1). It is a complex organ, that displays various essential functions in cooperation with its appendages, ranging from thermoregulation, sensory functions and hormone synthesis, as well as metabolism and maintenance of fluid balance, osmotic homeostasis, inter-individual communication by visual signals (pigments, hair), elaboration of special structures (claws, nails, hair, fins) and production of various specific substances (e.g. pheromones, antimicrobial peptides) through glandular secretion (Goldsmith 1991; Proksch et al. 2008; Rakers et al. 2010). Structure and function of fish skin is, in general, similar to that of vertebrates. The differences lie on the existence of an aquatic external milieu which determines the adaptation of the organism to the physical, chemical and biological properties, and also on the particular

evolutionary history of each species or taxonomic group. For these reasons, cutaneous lesions and associated diseases are more common in fish than in terrestrial vertebrates and constitute one of the primary factors which constrain skin structure of fish. These lesions are generally nonspecific and may be indicative of local disease, restricted to the integument, or a manifestation of a systemic disease (Groff 2001). Furthermore, an epidermal damage originates an osmotic stress and represents an open access for the infectious agents that can be life threatening for the fish (Ferguson 2006).

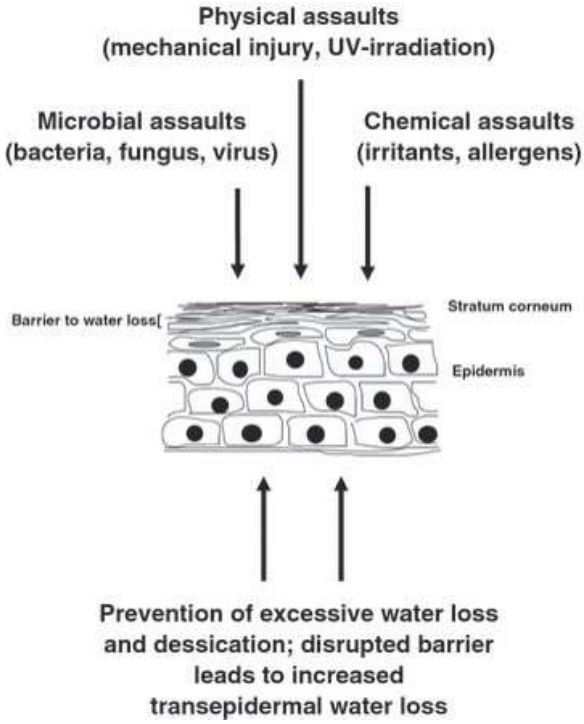

Figure 2.1. Representation of vertebrate's skin protective and preventive function (Proksch et al. 2008).

The general structure of the fish integument is common with what is found in higher vertebrates. It is composed of three principal layers: epidermis, dermis (or *corium*), and hypodermis (Harder 1976). The thickness and cellular composition of the three layers is, however, highly variable and dependent on various intrinsic and extrinsic factors, including species, development and life stage, location of the integument, season, sex, reproductive condition, nutrition, water quality, and general health status of the fish (Harder 1976). In teleosts, the skin can be divided into various strata with i) the epidermis being the most external layer and is composed of a stratified squamous epithelium containing the *stratum germinativum* (cuticle) and *stratum basale* (basement membrane) (Harder 1976; Whitear 2009; Whitear 1977); ii) the dermis, the intermediate stratum,

composed of the *stratum spongiosum*/ *stratum laxum* (external dermis) and *stratum compactum* (basal dermis) (Harder 1976); and iii) the hypodermis, the inner stratum or *tela subcutanea* (Figure 2.2) (Bullock & Roberts 1974).

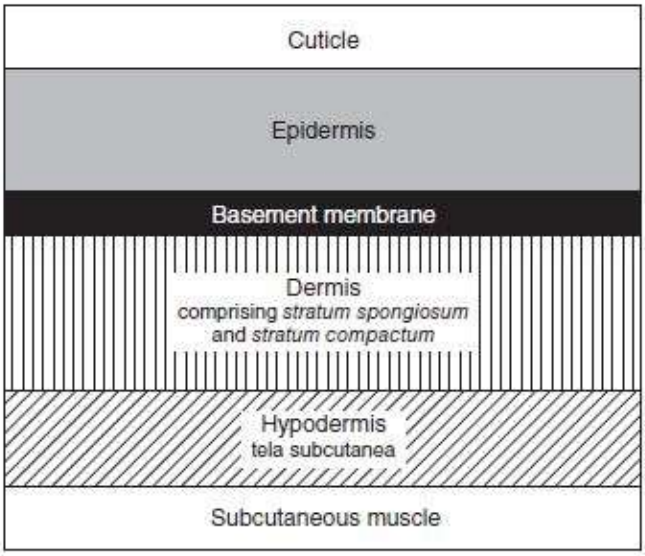

Figure 2.2. Schematic representation of the organization of teleost fish skin (Copied from Bullock & Roberts 1974*).*

The cuticle includes epithelial cells and mucous secretions, and it is a complex of cell protoplasm, sloughed cells and secreted mucus. The cuticle contains specific immunoglobulins and lysozyme, and free fatty acids and is the first antipathogen molecular barrier of the immune system. It has species specific physical consistency (Speare & Mirailimi 1992; Roberts 2012).

Malpighian cells are the most frequent cell type in the epidermis showing general rounded structure except the outermost ones, which are flattened horizontally. Scattered among the Malpighian cells, mucus-secreting cells are found in the epidermis of all teleosts. For instance, goblet cells are observable in the middle layer of the epidermis and, sometimes, near the basement membrane. However, as they approach to the surface their size and secretion content raises. Their abundance vary considerably with body location and species. Another type of cells may be found in some teleosts, which are known as club cells. These are big cells roundly shaped and can be found in the middle and lower layers of the epidermis. Therefore, the epidermis of fish is a stratified squamous epithelium covering the body surface and part of the tail and fins (Bullock & Roberts 1974; Roberts 2012). The viability and mitotic division capacity of the cells, even at the

outermost layer, contrasts with the non-viability of the outermost cells in mammals epidermis, make them more prepared for regeneration and healing (Ferguson 2006). Other cell types can be found in the normal epidermis but less frequently, like lymphocytes and macrophages, related to the immune system (Roberts 2012).

In the dermis, the *stratum spongiosum* is a loose network of collagen and reticulin fibers contiguous with the basement membrane of the epidermis (Craig et al. 1987; Harder 1976; Bullock & Roberts 1974). Pigment cells, like melanophores, xantophores and iridophores; cells of the scale beds and scales are present in this layer (Craig et al. 1987; Harder 1976; Roberts 2012; Ferguson 2006). Melanophores are responsible for the dark coloration, although they have the capacity of dispersing and concentrating their melanin pigment, changing color in response to external stimuli or stress. Xantophores are other type of pigment cells regularly present in teleosts which give the yellow pigmentation due to their organic solvent-soluble pigments content. The cells responsible for white and silver coloration in fish are called iridophores and contain purines, usually guanine, which are presented as plates of reflecting material with a variable thickness and arranged within the cell cytoplasm in parallel arrays (Bullock & Roberts 1974; Denton & Nicol 2009; Groff 2001). The scales are the primary component of the dermal skeleton in fish and, in teleosts, are calcified flexible plates which are partially included within the 'scale pockets' and oriented backwards (Harder 1976; Lagler et al. 1962; Roberts 2012). The most common scales are bony-ridge scales or elasmoid scales. These include two main types: cycloid and ctenoid scales. Cycloid scales are thin, translucent, circular disks with a smooth or entire exposed posterior margin. Ctenoid scales bear multiple comb-like or tooth-like projections, referred as ctenii, on their posterior external edge which makes them different from cycloid scales. Both types present growth rings on their surface that, in many species, can be related to the age of the fish. Scales are constituted by collagen fibers interspersed with a matrix of albuminoid materials with deposition of hydroxyapatite crystals. This fact makes scales a ready source of calcium to be reabsorbed during periods of starvation or pre-spawning in preference to the skeletal reserves (Harder 1976; Roberts 2012; Ferguson 2006). Great inter-species differences in teleost skin can be observed relative to the presence/absence of scales, since some species present no scales, others present numerous large eosinophilic club cells instead of scales and others have conical tubercle plates as a structural modification of elasmoid scales (Faílde et al. 2014; Zylberberg et al. 2003; Ferguson 2006). Besides this relevant description about the upper layer of the dermis, the lower layer (*stratum compactum*) has a relevant function in

the fish skin too. The relatively acellular nature and dense perpendicular collagen bundles with occasional elastic fibers composition of the basal dermis provides the structural integrity and tensile strength of the integument which counters or resists the contraction of skeletal muscle, resulting in flexural stiffness and more efficient excursion of the skeleton, and consequently more efficient locomotion (Long et al. 1996).

The hypodermis is less developed in fish and generally composed of a vascularized, loose adipose tissue that is often a common site for infection (Ferguson 2006). Lipids from this layer include various phospholipids and cholesterol esters which works as an energy reserve during inanition, a barrier to the diffusion of fluids, and a shock absorber (Mittal et al. 1976). Moreover, in certain fish, hypodermis may contain a mucous connective tissue named as mucochondroid tissue (Benjamin 1988). This tissue presents an abundant pale-staining glycosaminoglycan or glycoprotein matrix that contains a variable amount of fibroblasts, collagen, and blood vessels, being more frequent in locations that are associated with underlying bone (e.g. scales) and other sites of the integument (Groff 2001).

2.2. Cutaneous injuries and healing

Cutaneous lesions healing and resolution is highly controlled by temperature, and the process in fish is similar to that in higher terrestrial vertebrates, but faster, since epidermal covering and healing in fish is less affected by temperature, indicating the importance of epidermal integrity in this group. However, healing of the dermis is completely conditioned by temperature being, consequently, a slower process (Bullock & Roberts 1980; Anderson & Roberts 1975; Ferguson 2006; Roberts 1975; Roberts & Bullock 1976). Soon after an injury, a dark pigmentation generally occurs at the periphery of the lesion, there is a loss of intercellular connections between Malpighian cells, and re-epithelization starts immediately through recruitment and migration of Malpighian cells from the margins and over the surface of the dermal limit to the lesion (Groff 2001; Roberts 2012). Hyperplasia of mucous cells, followed by overproduction of mucus, may occur in the adjacent normal epidermis, and an exudate of blood and inflammatory cells immediately occupies the lesion. Once a single layer of epidermis is quickly formed, local hyperplasia of epidermal cells, proliferation of other cell types, increase of epidermal lymphocytes, and thickness reduction of the adjacent normal epidermis occurs (Mittal &

Munshi 1974; Quilhac & Sire 1999; Roberts 2012). The complete re-epithelization time is estimated around 4 to 6 hours (Mittal & Munshi 1974; Mittal et al. 1978). Thereafter, the slower process of epithelial cover reconstitution starts with a temperature-dependent normal mitotic proliferation, accompanied by formation of a fibrous scar and, then, reconstitution of the dermis (Bullock & Roberts 1980). Formation of dermal and hypodermal granulation tissue occurs within 72 to 96 hours after the injury. After approximately 25-35 days, epidermal and dermal/ hypodermal injuries are completely healed, respectively (Mittal & Munshi 1974; Mittal et al. 1978). Regeneration of elasmoid scales is performed in similar way as it happens in their ontogenesis and follows the closure of lesions (Sire & Géraudie 1984). In their ontogenesis, scales develop from dermal aggregations of cells (differentiated fibroblasts or scleroblasts) that form a scale-papillae/ scale-platellet within a dermal scale-pocket (Kobayashi et al. 1972; Sire & Géraudie 1984; Sire et al. 1997; Waterman 1970). The primitive scale anlage subsequently develops within the scale-papillae and is composed of multiple calcified layers, being the external layer formed by superficial scleroblasts and the internal layer/ basal plate formed by deep scleroblasts. Scleroblasts produce collagen fibers that are calcified by inotropic deposition of mineral within the interfibrillary matrix and the peripheral ones are responsible for the increase in diameter of the developing scale (Brown & Wellings 1969; Lanzing & Wright 1976; Schönbörner et al. 1979; Sire & Géraudie 1984; Sire et al. 1997; Zylberberg & Nicolas 1982). The fast growth of the scale proceeds from the nuclear zone, and occurs along the outer margins and beneath the scale. The nuclear zone is centrally located but assumes eccentric position near the anterior margin with enlargement of the scale. Their growth is generally continuous with some influences and restrictions by various intrinsic and extrinsic factors, like inactive periods such as winter, during periods of stress and calcium deficiency (e.g. reproduction) which can even lead to scale reabsorption, as previous reported (Harder 1976; Moyle & Cech 1988; Schönbörner et al. 1979). The repair and resolution of a skin injury may, however, be inhibited by the presence of contamination by bacteria in the ulcerated surface (Bullock & Roberts 1980). Usually, scar formation in the skin does not occur, appearing only with severe ulcerative lesions (Groff 2001).

2.3. Molecular and genetic basis of skin regeneration in fish

Despite the great importance of the fish skin as an immune barrier and as a fast regenerating tissue, little is known about the genes and molecular processes involved in the process of immune response and regeneration of this tissue, most available information coming from histological and pathological observations. Although in recent years, the number of molecular studies in the fish skin has increased (Casas et al. 2013; Vieira et al. 2011; Liu et al. 2013; Long et al. 2013; Micallef et al. 2012; Campinho et al. 2007), no study has been carried out before on the skin regeneration of brill and turbot. For instance, it is known that the Fibroblast Growth Factor (FGF) signaling pathway and the ectodysplasin (Eda) pathway are relevant for appendages development and likely for skin regeneration in some fish species (Rohner et al. 2009; Harris 2012; Harris et al. 2008; Mikkola & Thesleff 2003; Colosimo et al. 2005; Kondo et al. 2001). Moreover, immune-related genes are essential to control the progression of diseases, and in this regard, mediators like tumor necrosis factor (TNF) have shown to play a fundamental role for the innate and adaptive immune response of skin (Alvarez-Pellitero 2008). Finally, controlling osmotic imbalances is essential to keep body homeostasis, and members of the pituitary growth hormone family of peptide hormones (e.g. growth hormone receptor) work as crucial modulators of osmoregulation, growth, and metabolism (Pierce et al. 2007). Beyond these gene specific studies, a recent molecular study demonstrated the relevance of the first 72h *post* injury, which shows a majority and variety of molecular processes occuring together (Vieira et al. 2011).

2.4. Turbot and brill: biology and commercial interest

Brill (*Scophthalmus rhombus* (Linnaeus, 1758)) and turbot (*Scophthalmus maximus* (Linnaeus, 1758)) are two closely related congeneric flatfish (*Pleuronectiformes*) species (Froese & Pauly 2015; Wheeler 1992; Pardo et al. 2005a; Azevedo et al. 2008) based on their low genetic distance (Blanquer et al. 1992; Bouza et al. 2002), almost identical karyotype (Pardo et al. 2001) and low phylogenetic distance (Pardo et al. 2005b) (Figure 2.3). Morphology and function of the skin is very similar, but with a striking difference because brill presents cycloid scales (Muus & Nielsen 1999) while turbot has instead conical tubercle plates in their skin (Faílde et al. 2014; Zylberberg

et al. 2003) (Figure 2.4). Their distribution is very similar, being present in the East and Northeast Atlantic Ocean from Northwest Africa (Morocco) to the Arctic Circle. They are also present in the Baltic, Mediterranean and Black Sea (Froese & Pauly 2015). These flatfish have a demersal lifestyle characterized by living on sandy and muddy bottoms at varying depth (Besyst et al. 1999; Rodríguez Villanueva & Fernández Souto 2009). Moreover, they have similar ecological characteristics, with differences observed in the size at hatching, in the timing and duration of the spawn period, and in the optimal water conditions (Van der Hammen et al. 2013). The aquaculture production of these species started in the seventies (Daniels & Watanabe 2010) and has suffered a substantial increase, especially that of turbot, in the last few years, being 38.9% higher in 2013 than in 2011. Moreover, Portugal produced a remarkable amount of 4,400 tonnes in the year 2012, showing a strong and important production increase (FAO 2015).

*Figure 2.3. Phylogenetic distance between turbot and brill (*Pardo et al. 2005b*).*

Figure 2.4. Young adults turbot (A) and brill (B). Photos were taken during the experiment.

2.5. Objectives

The aim of this study is the analysis of the genetic differences in the skin response to injury between turbot and brill, 72h after a skin injury, using a previously designed immune-enriched 4x44k Agilent® oligo-microarray (Millán et al. 2010; Millán et al. 2011; Pardo et al. 2012).

The work was divided in various tasks, being i) screen of the microarray suitability for brill and for skin-related genes using bioinformatics; ii) skin scarification in turbot and brill and sampling after 72h; iii) samples preparation and selection of the ones with the best RNA and histological quality; iv) samples hybridization in the microarray; v) microarray data normalization; vi) analysis of the differences between the treatment and control gene expressions in turbot and in brill; vii) analysis of the gene expression differences between turbot and brill; viii) functional analysis of the most differentially expressed genes in turbot, in brill and between species; ix) microarray data corroboration through Real-Time PCR. A simplificated representation of the work is represented in the Figure 2.5.

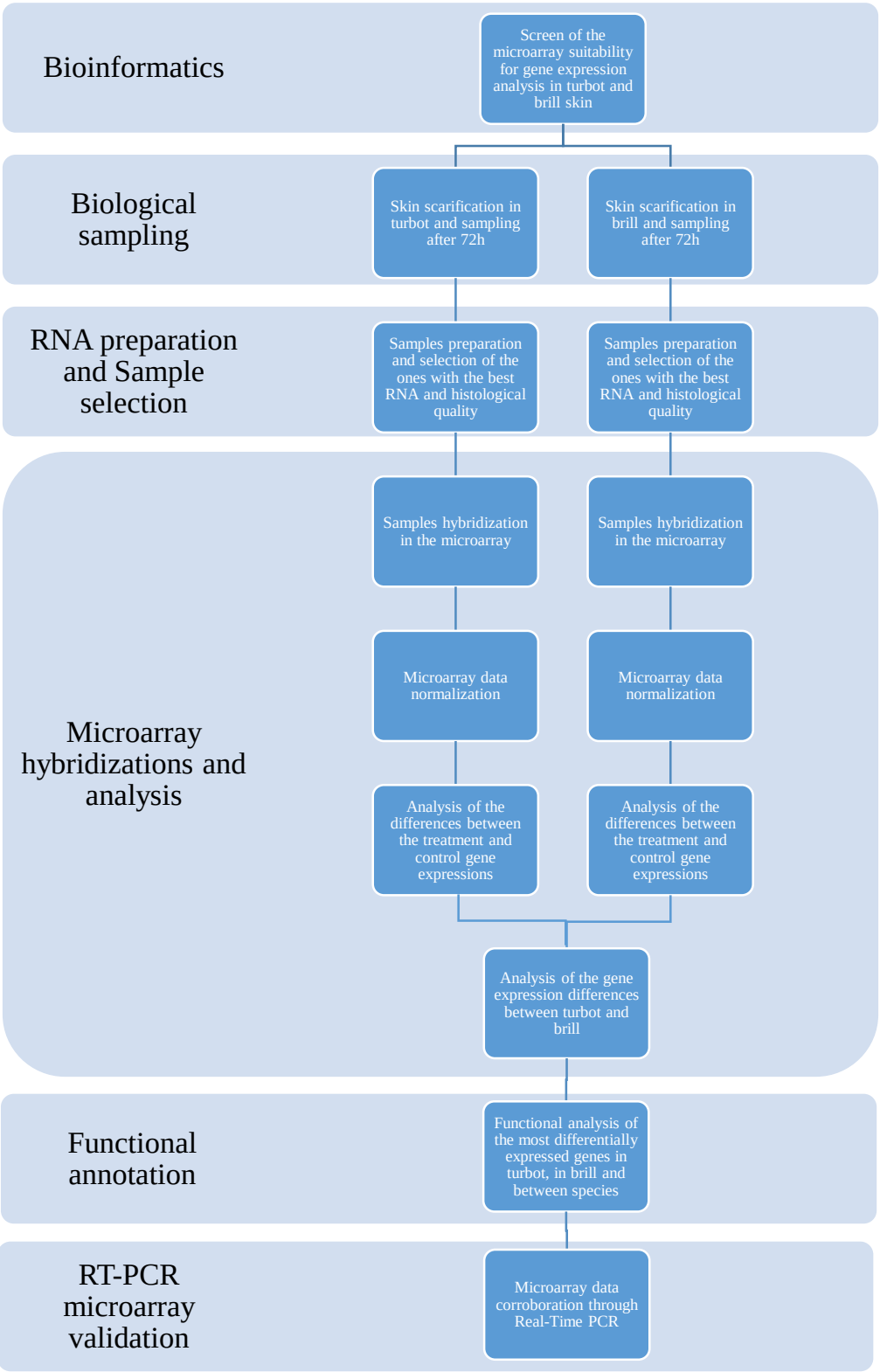

Figure 2.5. Flow diagram representing the project work plan.

3. MATERIALS AND METHODS

3.1. Bioinformatic strategy used to confirm the turbot microarray has a good representation of transcripts characteristic of skin

An initial sample of 1564 sequences (annex 1) from skin-related genes (NCBI database) selected from reported publications (Long et al. 2013; Micallef et al. 2012; Liu et al. 2013) was used to scan the Turbot 5 database (DB5) (Latest unpublished turbot transcriptomic database; Pereiro et al. 2012; Ribas et al. 2013) and the immuno-enriched oligo-microarray probes built for turbot (Turbot 4 database) in order to ascertain the microarray suitability for the skin gene expression analysis in turbot and in brill. First, the DB5 was scanned using a tblastn with the 1564 sequences against the database sequences. Second, the sequences from the DB5 which had homology with the 1564 sequences were BLASTed against the immuno-enriched oligo-microarray probes built for turbot using a nucleotide Megablast with the local alignment program BLAST-2.2.29+, since the turbot oligo-microarray was built with sequences from an older database (Turbot 4 database (DB4)). The e-value cut off and the minimum identity percentage applied for the tblastn was $\leq$ 9e-20 and $\geq$ 80%, respectively. The minimum identity percentage applied for the Megablast was $\geq$ 95%.

3.2. Biological sampling

The skin of healthy young adult brill (n = 6; age: 11 months; weight: 176,8 ± 42,02 g; length: 22,58 ± 3,353 cm) and turbot (n = 6; age: 30 months; weight: 1150 ± 155,5 g; length: 36,92 ± 1,656 cm), maintained under standard culture and feeding conditions at IFAPA Centro Agua del Pino (Huelva, Spain) and at Cluster de la Acuicultura de Galicia (A Coruña, Spain) facilities, respectively, was scraped with the blunt side of a knife on the upper side of the lateral line in order to remove the scales and epidermis. Only the epidermis and superior dermis layers from turbot skin and the scales from brill skin (together with the epidermis and superior dermis layers) were scraped off and the damaged area corresponded approximately to a square of 2 cm^2 at the middle of the body relative to the tail. The individuals were keep in normal culture and feeding conditions for 72h. Then, 4 skin samples from each individual were collected. Two skin samples

(one from the injured side and the other from intact skin) were obtained and stored in RNA later (1 piece of tissue per 5 volumes of RNA later) for RNA extraction and subsequent RNA quality evaluation. The other 2 samples (one from injured and another from normal skin) of skin and muscle (~1cm^3) were obtained and stored [brill samples in 4% PFA (2 g of PFA, 5 ml of H2O, one drop of NaOH (0.5-1 M), 45 ml of PBS, and pH adjusted to 7.4 with HCl. One volume of tissue per 5-10 volumes of fixative was used), and turbot samples into 4% formol (71 ml of acid picric supersaturated in distilled water, 24 ml of formaldehyde, and 5 ml of acetic acid. One volume of tissue per 5-10 volumes of fixative was used.)] for histological quality analysis.

3.3. RNA preparation and Sample selection

Pooled tissues were ground to a fine powder in a mortar and pestle with liquid nitrogen and finally stored at -80ºC until used for RNA extraction. Total RNA was extracted from pooled tissues of control and treatment using TRIZOL reagent (Life Technologies) according to manufacturer's recommendations. All extractions were performed by the same researcher.

Six individuals (3 brill and 3 turbot) were excluded from the microarray analysis because either, 1) they failed to pass the quality threshold for RNA quality (Bioanalyser, Bonsai Technologies) and quantification (NanoDrop® ND-1000 spectrophotometer, NanoDrop® Technologies Inc) analysis or 2) in light microscopy analysis of thin sections of skin stained with haematoxilin-eosin (H-E) damage was more or less extensive than the superior dermis.

3.4. Microarray hybridizations and analysis

Total RNA selected from quality and quantification analysis was reverse transcribed into cDNA. The double strand cDNA was then transcribed into cRNA and labelled with Cyanine 3 dye for microarray hybridization (Figure 3.1). A solid-phase (glass) 1x3", 4x44K Agilent® oligo-microarray slide (Millán et al. 2010; Millán et al. 2011; Pardo et al. 2012), including 4 microarrays per slide and 45220 spots per microarray (43803 60-mer oligo-probes, with 3425 duplicated probes and some repeated genes with unknown sequence direction, plus Agilent® RNA spike-in controls), designed using the

turbot 4 Database ESTs from spleen, liver and head kidney was used to evaluate gene expression profiles after 72h *post* skin scraping. Two slides were used in the experiment, one per species, using a 1-color labelling approach. On each slide, 4 microarrays (1 control + 3 individual samples) were used. Hybridizations were performed by loading the labelled cRNA and the corresponding reagents onto the slides at the Universidade de Santiago de Compostela Functional Genomics Platform using Agilent® Gene Expression Analysis. The temperature used for hybridizations was 65ºC for both species. All work was carried out on the same day and by the same researcher.

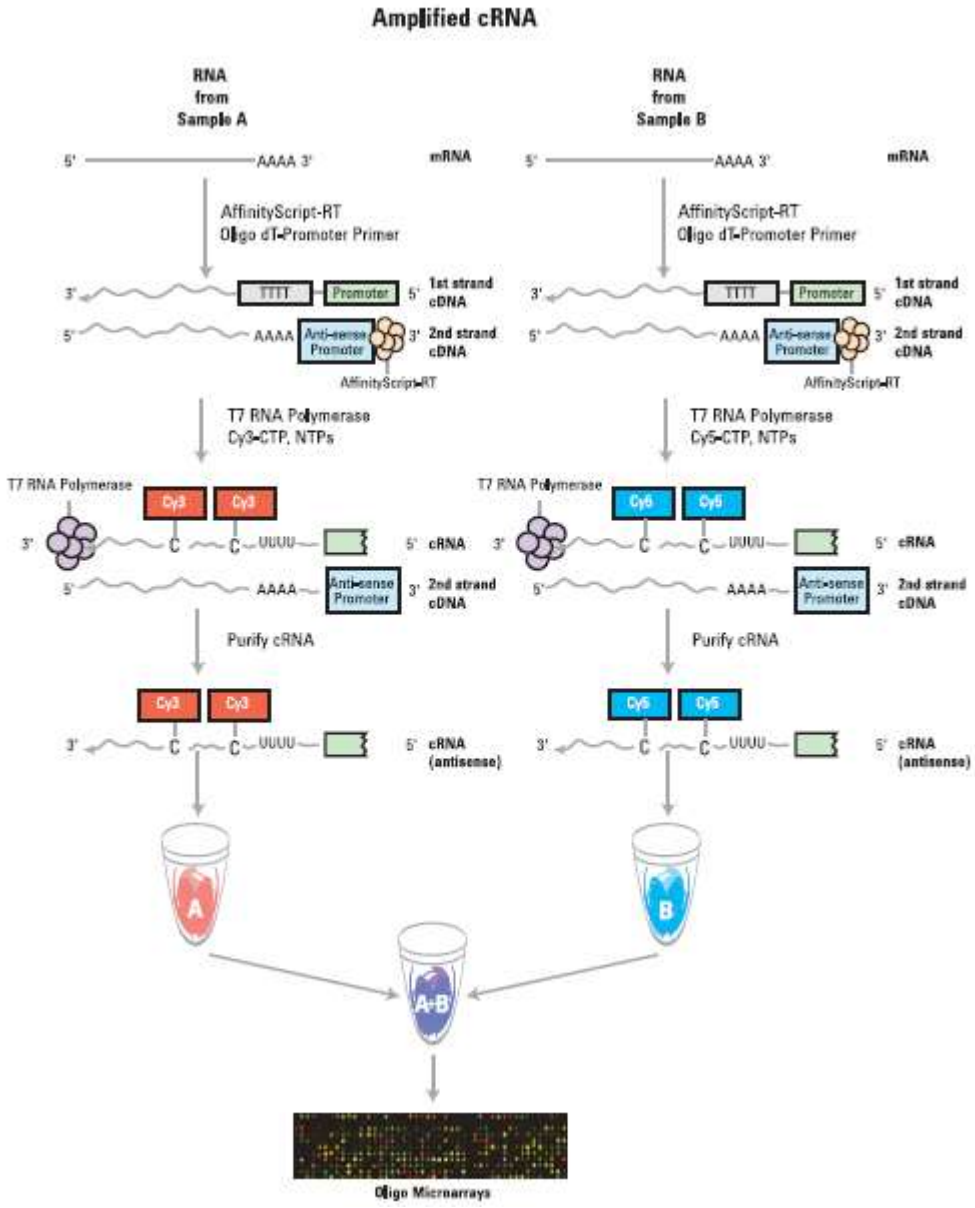

Figure 3.1. Schematic representation of cRNA amplification procedure for a two-color microarray experiment. For a one-color microarray experiment, only the Cyanine 3-labelled (Cy3-CTP) sample is produced and hybridized (from Agilent Technologies 2014).

Since normality of the log (log-normality) microarray signal is assumed, the log2 transformation of the ratios treatment/control was used in the statistical analysis. Normalization within each microarray was carried out using the LOESS method, which assumes that most genes in the microarray are not differentially expressed in relation to the control. Normalized data were organized into .mev files using a homemade R program for statistical analysis with the MultiExperiment Viewer (MeV) program (Saeed et al. 2006). An initial filter of fluorescent signal (<200 fluorescence units) was applied to avoid the presence of false-positives due to background signal. In the statistical analysis, two different criteria were used to identify Differentially Expressed (DE) genes in each species, in response to the skin injury: (a) genes with log2 ratios ≥ 2 or ≤ -2 in at least one of the biological replicates for up- and downregulated genes, respectively, and (b) genes which deviated from the null hypothesis (mean log2 ratio = 0) using t tests at $P < 0.005$. Another two different criteria were used to identify DE genes between species: (a) genes with mean log2 ratio difference between species ≥ 2, and (b) genes which showed statistical differences in the mean log2 ratio between species using t tests at $P < 0.005$.

3.5. Functional annotation of the most differentially expressed genes

Putative functions of the genes represented on the Tables 4.3 – 4.8 (62 genes) were accessed by their gene name annotated in the microarray probes and searched in the UniProt and NCBI databases (http://www.uniprot.org/; http://www.ncbi.nlm.nih.gov/). The represented genes were classified into functional categories, and their term enrichment analyzed through the DAVID program (Huang et al. 2009b; Huang et al. 2009a). Official gene symbols of the represented genes and all available species present in the DAVID database were used as a gene list and as a background, respectively, to test enriched functions. The default p-value given by the DAVID program is 0.1 but since the genes list used with known putative functions was small, a less stringent p-value cut-off was applied, and a cut-off of 0.2 was used.

3.6. RT-PCR microarray validation

To validate microarray results by RT-PCR we evaluated the suitability of a set of 19 genes, used for microarray validation in previous studies in the turbot, for the brill and turbot RNA from skin samples (Millán et al. 2011; Pardo et al. 2012; Robledo et al. 2014). The first step was to ascertain the performance of the primers set in the brill. A PCR was performed with the 19 primer pairs in the RNA from brill skin samples, using the amplification parameters reported for turbot. After amplification and quality evaluation of the PCR, 17 of the primer pairs were selected for use in brill RT-PCR and all 19 primer pairs were used for turbot RT-PCR. Primer pairs were excluded from the initial 19 pairs due to poor amplification in brill RNA from skin samples, and the lack of fluorescent signal in the microarray hybridization with turbot or brill RNA from skin samples. Finally, primer pairs for amplification of 9 genes were selected to validate the turbot microarray results and 6 genes were selected to validate the brill microarray results throught RT-PCR analysis (Table 3.1). Ribosomal Protein S4 (Official gene symbol: RPS4) was used as the housekeeping gene for RT-PCR analysis as it has previously been shown to have consistent expression in turbot (Robledo et al., 2014). RNA (~1 µg) was reverse transcribed into cDNA using AffinityScript Multiple Temperature cDNA Synthesis kit according to the supplier's protocol (AGILENT TECHNOLOGIES). The RT-PCR analysis was carried out in a MX3005P thermocycler (STRATAGENE) using ~1 µl of cDNA in 20 µl reaction following the Brilliant III Ultra-Fast SYBR® Green QPCR Master Mix (AGILENT TECHNOLOGIES) as described by Millán et al. (2011).

Table 3.1. List of primers used for RT-PCR in turbot and brill.

DB 4 ID	Gene name	Accession number	Primer F (5' -> 3')	Primer R (5' -> 3')	Product lenght (bp)	Temp (ºC)	Efficiency (%)
R4_26907	Dact[1]	KR019999	TCAGAGGGCAAAAATGGGCT	ACTTCAGTGGGCTTCCTGTG	144	59,89	92,01
R4_21653, R4_5341, R4_7967	dnmt1[1, 2]	KR019994	GGAGTACGCGCCCATCTTT	GTCCTCCGTGAAGCAGTTGA	169	59,97	90,86
R4_16440	hh1[1]	KR020002	AGAGAGCCAAGTATCGGAGG	ATCCTTCAGCCTTCAGAGCC	132	58,30	89,33
R4_2297	rdh3[1, 2]	KP658395	CTGACGACCACACACCTTGA	GCGACTCCAGCATTGTTCAC	119	59,83	90,03
R4_22211, R4_6520	sox17[1]	JQ403638	TGTTCGGGAAGCAGGTGAAAGGT	CTTGTTGCCATTTTAGGGGACAGT	92	58,44	87,95
R4_10661, R4_8329, R4_10661	upg2[1, 2]	FE944840	CAGGAGTTTCTGTCCAGGTTTGAG	ATTGGCGATGATGATGACGGTTC	126	59,20	93,00
R4_64278	adh6[1, 2]	FE952304	GCTTATCGCTGGACGCACTTG	TGGCTTCACTGACAACAACGC	242	59,35	96,90
R4_114	rps4[1, 2]	FE943563	CAACATCTTCGTCATCGGCAAGG	ATTGAACCAGCCTCAGTGTTTAGC	143	59,70	101,70
R4_60836	dmrt2[1, 2]	KP677565	GACTTTCTGTCCAAGCCCCT	GGGCGTGGGTCTTTTCAGTA	91	59,60	88,92

[1] Primer used in turbot. [2] Primer used in brill.

3.7. Histological quality analysis

To analyze the quality of tissues for the final selection of samples, brill samples were fixed in 4% PFA (2 g of PFA, 5 ml of H2O, one drop of NaOH (0.5-1 M), 45 ml of PBS, and pH adjusted to 7.4 with HCl. One volume of tissue per 5-10 volumes of fixative was used), and turbot samples into 4% formol (71 ml of acid picric supersaturated in distilled water, 24 ml of formaldehyde, and 5 ml of acetic acid. One volume of tissue per 5-10 volumes of fixative was used). Tissue samples were processed by first dehydrating in alcohol, followed by clearing in xylene and embedding in paraffin. Thin sections (2-3 µm) were prepared, mounted on glass slides and stained with haematoxylin-eosin (H-E) (Bancroft & Gamble 2008).

4. RESULTS AND DISCUSSION

4.1. Bioinformatics analysis

An initial sample of 1564 sequences (annex 1) was used to scan the Turbot 5 database (DB5) (Latest unpublished turbot transcriptomic database; Pereiro et al. 2012; Ribas et al. 2013) and the immuno-enriched oligo-microarray probes built for turbot (Turbot 4 database) as described in the subsection 3.1 of Materials and Methods. A total of 584 genes (~37% of the initial sample) were present in DB5 and 326 (~21% of the initial sample) were present in the oligo-microarray (Figure 4.1; annex 2). A notable presence of skin-related genes in both the DB5 and the microarray is observable, especially for the turbot microarray, since it was made and enriched with immune-related tissue genes (Millán et al. 2010; Millán et al. 2011; Pardo et al. 2012).

A preliminary bioinformatic analysis was made to ascertain the suitability of the turbot oligo-microarray for gene expression analysis in brill. However, the number of brill sequences available on the NCBI database was scarce which meant statistical analysis could not be used and, therefore, this comparative sequence analysis was excluded from the thesis presentation.

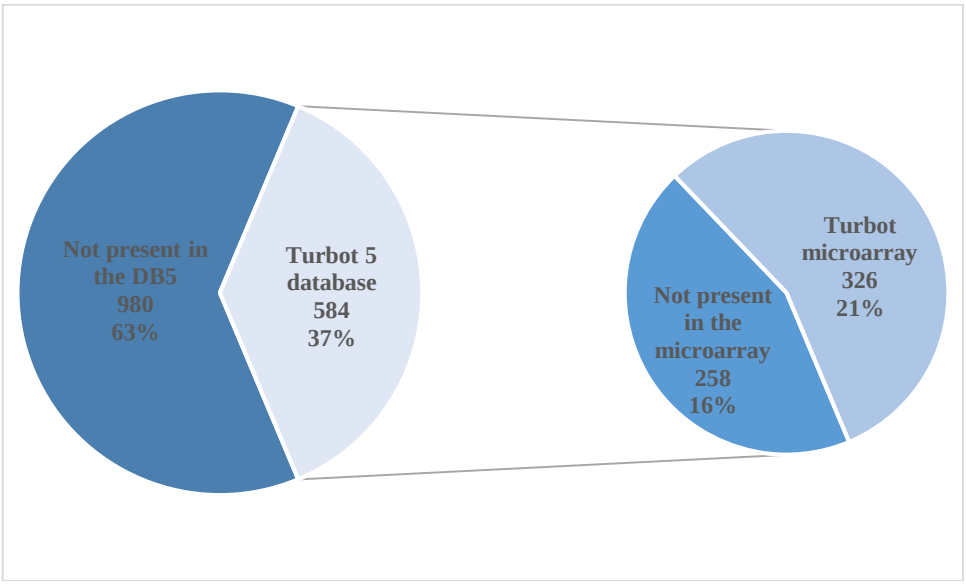

Figure 4.1. Skin-related genes from previous studies (1564 genes) detected in the turbot database and in the turbot oligo-microarray.

4.2. Microarray gene expression analysis

Six individuals were chosen for gene expression analysis (3 per species) considering their best RNA and/or skin section sample qualities. Regarding to RNA quality, samples with the best RIN number (Schroeder et al. 2006) were considered to be included (Figures 4.2 and 4.3). Relatively to skin section samples, the level of skin damage was evaluated and samples with moderated skin damage (removal of epidermis and superior dermis) and with as less artefacts as possible were considered apt for the study. The number of genes with consistent fluorescent signal (> 200 f. u.) in each species was 15,739 in turbot, 12,393 expressed genes in brill. The number of common genes with consistent signal in both species was 10,065 (Table 4.1). As expected, a considerable number of expressed genes in turbot is observable. Nevertheless, a notable number of genes expressed for brill in the turbot microarray is evidenced. These results, together with the notable presence of skin-related genes in the microarray mentioned above, shows a strong feasibility in the evaluation of brill genes in the microarray. Moreover, it demonstrates and confirms the suitability of the turbot immune-enriched microarray for both brill and skin-related genes, once the analysed genetic sample was exclusively RNA from skin of these two species. Another fact can be stated with the appreciable quantity of shared expressed genes in both species which is the corroboration of the genetic proximity between turbot and brill, determined in previous studies (Bouza et al. 2002; Blanquer et al. 1992).

Table 4.1. Expressed genes with consistent fluorescent signal (>200 fluorescent units) in the 4X44k turbot oligo-microarray.

Total expressed genes

	Turbot	**Brill**	**Turbot and Brill**
Microarray	15739	12393	10065
Fish skin genes[1]	218	206	176
Relevant genes[2]	72	49	43
Candidate genes for scale regeneration[3]	3	2	1

[1] genes from the initial sample of fish skin genes. [2] public known genes with relevant functions in the skin. [3] genes from the Fibroblast Growth Factor signaling pathway and Ectodysplasin pathway.

DE genes in each (in response to skin injury) and between species were identified by using two different criteria as described in the subsection 3.4 of Materials and Methods. The number of DE genes was 1750 for brill and 1461 for turbot (annex 3 and 4, respectively), in response to skin injury. A total of 885 genes showed differences in expression between species (Table 4.2; annex 5). Tables with the 10 DE genes with highest absolute log ratio in each species response to skin injury, highest DE difference between species and available putative function in the UniProt and NCBI databases (http://www.uniprot.org/; http://www.ncbi.nlm.nih.gov/) are represented in the Tables 4.3 and 4.4, respectively. Surprisingly, brill shows higher expression than turbot and the number of differently expressed genes indicates observable differences in genes expression response to skin injury. However, genes expression values in turbot have a higher standard deviation between biological replicates (individuals) than in brill. This fact may cause a considerable variability between the gene expression values of the individuals, resulting in a less rigorous analysis and results in turbot. Higher variability in gene expression values between turbot individuals may be associated with the observable difference in the skin structure relatively to brill, since turbot tubercles are, most often, isolated and randomly distributed, comparing to brill scales which are more frequent and less randomly distributed (Zylberberg et al. 2003). Therefore, a different arranjement of the appendices in the fish skin may result in a different skin response to injury.

Table 4.2. Differentially expressed (DE) genes within and between species.

	Turbot	**Brill**	**Between species**
Microarray	1461	1750	885
Fish skin genes[1]	18	32	20
Relevant genes[2]	8	4	4
Candidate genes for scale regeneration[3]	-	1	1

[1] genes from the initial sample of fish skin genes. [2] public known genes with relevant functions in the skin. [3] genes from the Fibroblast Growth Factor signaling pathway and Ectodysplasin pathway.

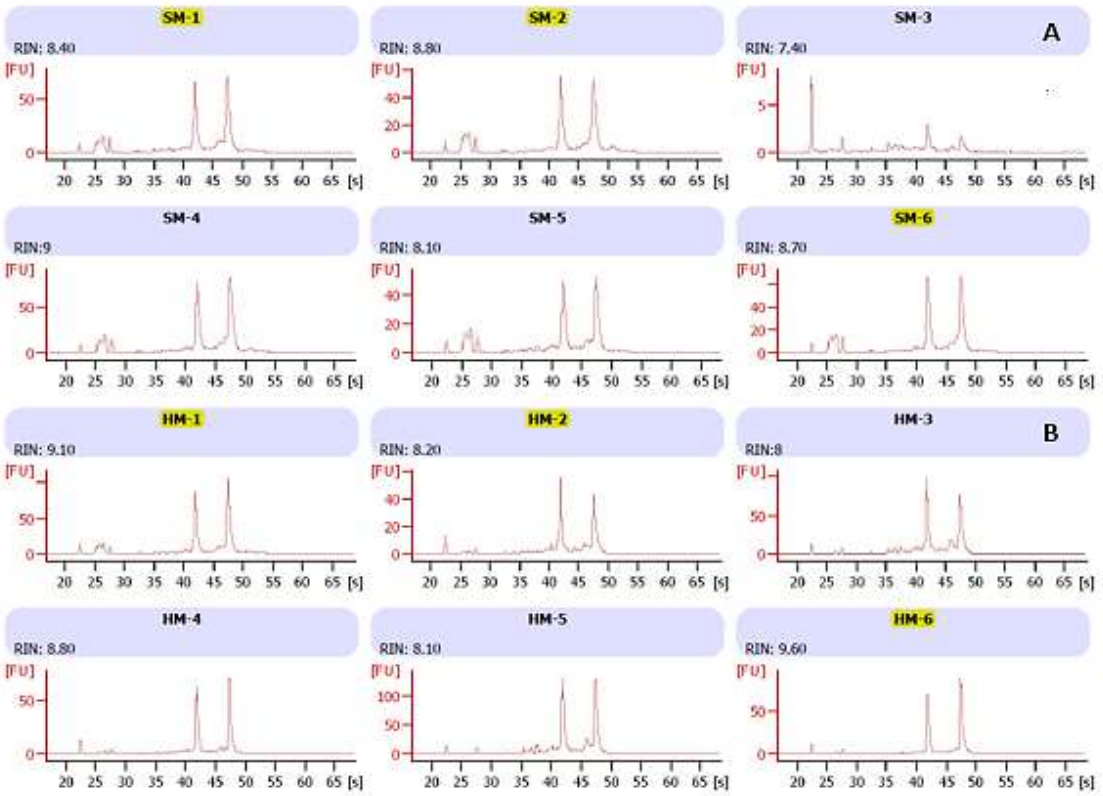

Figure 4.2. Turbot sampled RNA quality analysis. 'SM' indicates control samples and 'HM' indicates treatment samples. Yellow marked samples represent the chosen individuals for this study.

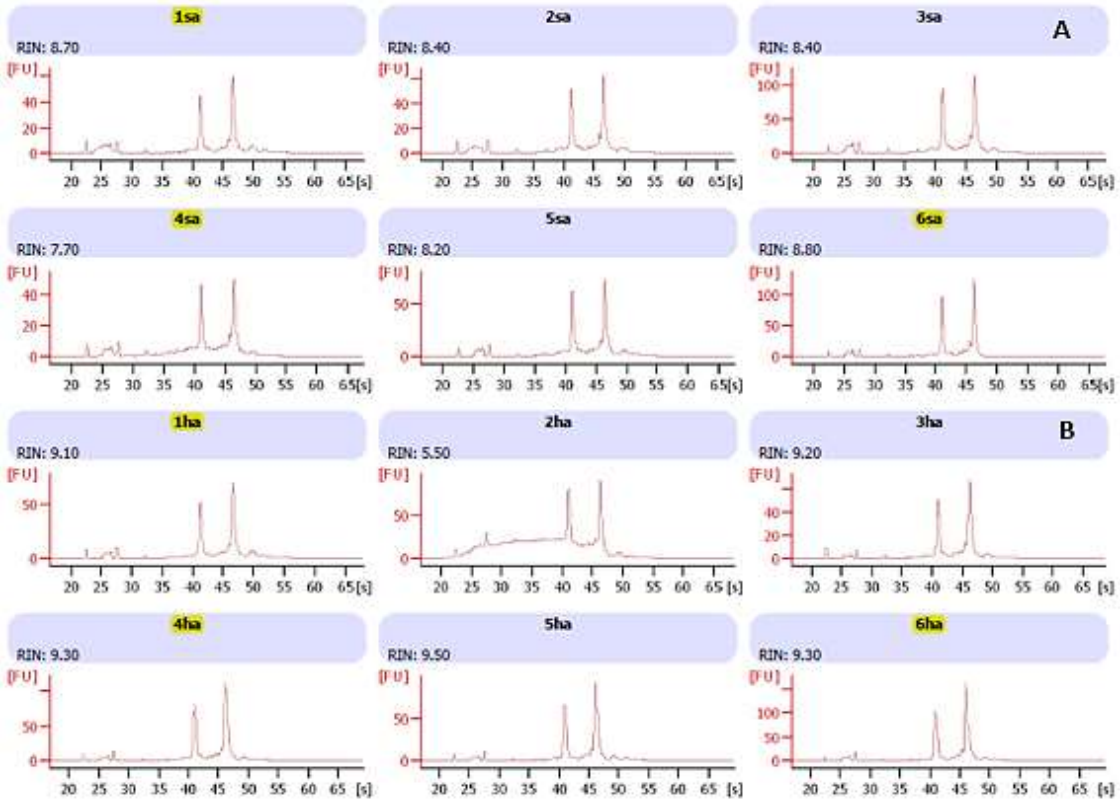

Figure 4.3. Brill sampled RNA quality analysis. 'sa' indicates control samples and 'ha' indicates treatment samples. Yellow marked samples represent the chosen individuals for this study.

Table 4.3. "Top 10" highest DE genes in each species response to skin injury, identified from the microarray.

Probe Name	Gene description	Putative function	Mean Log_2 ratio	P value
		Turbot		
R4_53611	Ecto-ADP-ribosyltransferase 5	Catalytic activity: Protein ADP-ribosylation (the transfer, from NAD, of ADP-ribose to protein amino acids).	6,120	0,006
R4_58772.1	Tumor necrosis factor receptor superfamily member 6B	Apoptotic programmed cell death: Protects against apoptosis.	5,316	0,004
R4_51569.1	Interleukin-8	Chemotactic factor: Attracts neutrophils, basophils, and T-cells. Neutrophil activation.	4,897	0,034
R4_31059r	M17 homologue	Immune response.	5,015	0,016
R4_13016r	Cell cycle checkpoint control protein RAD9A	Cellular response to DNA damage stimulus.	4,598	0,012
R4_51611.1	L-threonine dehydrogenase	Pyridoxine biosynthetic process (macronutrient metabolism).	-3,853	0,012
R4_2851.1	DnaJ homolog subfamily B member 14	Co-chaperone with HSPA8. Promotes the degradation of misfolded transmembrane proteins.	-3,853	0,045
R4_18066r	Proline arginine-rich end leucine-rich repeat protein	Extracellular matrix structural constituent. May anchor basement membranes to the underlying connective tissue.	-3,832	0,049
R4_13540r	ABI family, member 3 (NESH) binding protein	Extracellular matrix organization. Positive regulation of cell-substrate adhesion.	-3,877	0,085
R4_10398	Matrix Gla protein	Regulation of bone mineralization. Inhibition of bone formation.	-3,964	0,043
		Brill		
R4_10711r	S100-A6	Calcium sensor and modulator. Reorganization of the actin cytoskeleton and cell motility.	5,330	0,019
R4_2305	Cell division protein kinase 1	Apoptotic process. Cell division. Epithelial cell differentiation. Mitotic nuclear division.	3,937	0,002
R4_7618r	Topoisomerase (DNA) II alpha	Mitotic cell cycle.	3,768	0,003
R4_9416	Serpin peptidase inhibitor, clade E (nexin, plasminogen activator inhibitor type 1), member 1	Blood coagulation. Circadian rhythm. Extracellular matrix organization. Fibrinolysis. Gene expression.	3,722	0,013
R4_11656r	Cell division cycle associated 7-like	Positive regulation of cell proliferation.	3,596	0,002
R4_44196	Ubiquitin specific peptidase 22	Chromatin organization.	-3,690	0,001
R4_13221.1	Mucin 5, subtype B, tracheobronchial-like	Cellular protein metabolic process.	-3,707	0,049
R4_10572r	Collagen, type X, alpha 1	Collagen catabolic process. Extracellular matrix disassembly and organization. Skeletal system development.	-4,337	0,021
R4_53735	Troponin I, cardiac muscle	Muscle filament sliding.	-3,651	0,014
R4_44336	Smoothelin, like	Regulation of contractile properties of both striated and smooth muscles.	-3,173	0,007

Table 4.4. "Top 10" most differently expressed genes between species identified from the microarray.

Probe Name	Gene description	Putative function	Mean Log_2 ratio (brill)	Mean Log_2 ratio (turbot)	Mean Log_2 ratio dif	P value
R4_7618r	Topoisomerase (DNA) II alpha	Mitotic cell cycle.	3,768	-1,037	4,806	0,001
R4_2305	Cell division protein kinase 1	Apoptotic process. Cell division. Epithelial cell differentiation. Mitotic nuclear division.	3,937	-0,772	4,708	0,000
R4_47782	Aurora kinase B	Mitotic cell cycle. Protein autophosphorylation.	3,555	-0,591	4,146	0,001
R4_10496r	Stathmin	Regulation of the microtubule (MT) filament system. Control of the learned and innate fear.	2,639	-1,483	4,122	0,008
R4_485.2	Complement factor D/ adipsin and kallikrein-like serine protease	Blood coagulation. Complement activation. Innate immune response. Platelet activation and degranulation. Proteolysis.	2,991	-1,005	3,996	0,066
R4_12817.2	Heparin-binding EGF-like growth factor	Innate immune response. Muscle organ development.	-1,575	2,365	-3,939	0,003
R4_4183	DNA-directed RNA polymerase II subunit H	DNA repair. Gene expression. Innate immune response. Regulation of gene expression, epigenetic. RNA splicing. Somatic stem cell maintenance. Viral process.	-2,956	2,646	-5,601	0,010
R4_13286	6-phosphofructo-2-kinase/ fructose-2,6-biphosphatase 3	Canonical glycolysis. Carbohydrate metabolic process. Energy reserve metabolic process. Gluconeogenesis. Glucose metabolic process. Intracellular signal transduction.	-0,338	3,681	-4,020	0,050
R4_11425	Calpain-3	Apoptotic process. Muscle cell cellular homeostasis. Muscle organ development. Signal transduction.	-0,611	3,316	-3,926	0,011
R4_65007	Peptidoglycan recognition protein L1	Negative regulation of gene expression.	-0,028	4,267	-4,296	0,037

The 326 genes from the initial sample of fish skin genes, which are present in the microarray, were specially considered to check their expression. In turbot, 218 skin genes showed consistent expression and 18 were DE in response to skin injury and in brill, 206 genes expressed and 32 were DE in response to skin injury. In both species, 176 genes were expressed and 20 were DE between them (Tables 4.1 and 4.2). Lists of the 10 highest DE genes within and between species were obtained from these 326 genes (Tables 4.5 and 4.6, respectively).

Table 4.5. "Top 10" most DE genes in each species response to skin injury, identified from the fish skin genes sample.

Accession number	Probe Name	Gene description	Putative function	Mean Log_2 ratio	P value
Turbot					
NP_001032454	R4_10715	6-phosphofructo-2-kinase/ fructose-2,6-biphosphatase 4, like	Fructose metabolic process.	1,701	0,076
NP_956047	R4_269r	Calponin-2	Cytoskeleton organization.	1,690	0,081
NP_998231	R4_32855	Hexokinase 2	Canonical glycolysis. Carbohydrate metabolic process. Glucose metabolic process. Glucose transport. Transmembrane transport.	1,639	0,045
NP_001122153	R4_2564	Vinculin	Blood coagulation. Cell adhesion. Cell-matrix adhesion. Movement of cell or subcellular component. Muscle contraction. Negative regulation of cell migration. Platelet activation and degranulation.	1,066	0,002
NP_956267	R4_20869r	PREDICTED: similar to ubiquitin specific protease 14 isoform 1	Cysteine-type endopeptidase activity. tRNA guanylyltransferase activity.	1,008	0,001
NP_001108199	R4_12123	Ring finger protein 122-like	Zinc ion binding.	-1,639	0,045
NP_001002667	R4_6475	Solute carrier family 25, member 36a	Transmembrane transport.	-2,023	0,007
NP_001018337	R4_1116	Glutathione peroxidase	Oxidation-reduction process. Response to oxidative stress.	-2,098	0,024
NP_001025256	R4_15761r	Dermatopontin	Cell adhesion. Collagen fibril organization. Negative regulation of cell proliferation.	-3,313	0,036
NP_001139254	R4_10997	Collagen, type V, alpha 2-like	Axon guidance. Collagen catabolic process. Extracellular matrix disassembly and organization.	-3,365	0,029
Brill					
NP_997729	R4_2305	Cell division protein kinase 1	Apoptotic process. Cell division. Epithelial cell differentiation. Mitotic nuclear division.	3,937	0,002
NP_001017574	R4_11656r	Cell division cycle associated 7-like	Positive regulation of cell proliferation.	3,596	0,002
NP_997732	R4_2288	Predicted ATPase involved in replication control, Cdc46/ Mcm family	DNA replication. Intein-mediated protein splicing.	3,480	0,006
NP_001032780	R4_9715	Ubiquitin carrier protein	Positive regulation of BMP signaling pathway. Protein monoubiquitination. Retrograde transport, endosome to Golgi.	3,284	0,001
NP_944595	R4_10078r	DNA replication licensing factor mcm4	DNA strand elongation involved in DNA replication. G1/S transition of mitotic cell cycle. Mitotic cell cycle.	2,694	0,004
NP_001103872	R4_11422r	UDP-glucose dehydrogenase	Cellular glucuronidation. UDP-glucose metabolic process.	2,502	0,006
NP_001133614	R4_1536	EH domain-containing protein 3	Blood coagulation. Nucleic acid binding.	2,240	0,000
NP_001187576	R4_3056r	RNA polymerase II, polypeptide H-like	DNA repair. Innate immune response. mRNA splicing. Negative regulation of gene expression, epigenetic. Positive regulation of viral transcription. Somatic stem cell maintenance.	1,998	0,002
NP_001070097	R4_11114	ARMET protein encoding gene	Dopamine metabolic process. Neuron cellular homeostasis. Neuron projection development.	1,991	0,000
XP_002667793	R4_25707r	NAD(P) transhydrogenase	Cellular metabolic process. Hydrogen ion transmembrane transport. Oxidation-reduction process. Tricarboxylic acid cycle.	-2,176	0,013

Table 4.6. "Top 10" most Differently Expressed genes between species identified from the fish skin genes sample.

Accession number	Probe Name	Gene description	Putative function	Mean Log_2 ratio (brill)	Mean Log_2 ratio (turbot)	Mean Log_2 ratio dif	P value
NP_997729	R4_2305	Cell division protein kinase 1	Apoptotic process. Cell division. Epithelial cell differentiation. Mitotic nuclear division.	3,937	-0,772	4,708	0,000
NP_001017574	R4_11656r	Cell division cycle associated 7-like	Positive regulation of cell proliferation.	3,596	-0,270	3,866	0,001
NP_001032780	R4_9715	Ubiquitin carrier protein	Positive regulation of BMP signaling pathway. Protein monoubiquitination. Retrograde transport, endosome to Golgi.	3,284	-0,454	3,738	0,000
NP_997732	R4_2288	Predicted ATPase involved in replication control	DNA replication. Intein-mediated protein splicing.	3,480	-0,096	3,576	0,003
NP_001025256	R4_15761r	Dermatopontin	Cell adhesion. Collagen fibril organization. Negative regulation of cell proliferation.	-0,019	-3,313	3,293	0,041
NP_001139254	R4_10997	Collagen, type V, alpha 2-like	Axon guidance. Collagen catabolic process. Extracellular matrix disassembly and organization.	-0,116	-3,365	3,249	0,031
NP_944595	R4_10078r	DNA replication licensing factor mcm4	DNA strand elongation involved in DNA replication. G1/S transition of mitotic cell cycle. Mitotic cell cycle.	2,694	-0,216	2,911	0,002
NP_878286	R4_1127.1	Glutamine synthetase	Cellular amino acid biosynthetic process. Glutamate catabolic process. Neurotransmitter uptake.	1,179	-1,628	2,808	0,032
NP_999924	R4_307	Asparaginyl endopeptidase	Innate immune response. Innate immune response. Vitamin D metabolic process	1,861	-0,143	2,003	0,001
NP_001032454	R4_10715	6-phosphofructo-2-kinase/ fructose-2,6-biphosphatase 4, like	Fructose metabolic process.	-0,708	1,701	-2,410	0,045

Relevant genes regarding to: i) cellular cycle, division, proliferation and differentiation; ii) dermal skeleton development; iii) regeneration, growing and development of a tissue; iv), energy production metabolism; v) osmotic stress; and vi) immune response, were identified and their expression profiles specifically analysed considering their role in skin regeneration (Table 4.7). Beside these relevant genes, genes from two pathways regarding to scales formation, reported in a recent study (Casas et al.

2013), were screened for the expression in the microarrays of both species. The number of expressed genes from the Fibroblast Growth Factor signaling Pathway and the Ectodysplasin Pathway in the microarrays are represented in the Tables 4.1 and 4.2, and their respective expression within and between species in the Table 4.8. The pathway genes symbols and names were taken from STRING public database (http://string-db.org/).

The significantly expressed genes represented in the Tables 4.3 – 4.8 were classified to their Gene Ontology terms (GO ID) and KEGG PATHWAYS in order to determine which functions are represented in each species and which ones differ between them. Overall, 7 genes for turbot, 3 for brill and 8 between species could not be associated with at least a GO term. Functions regarding to: i) regulation of DNA metabolic process, ii) cellular response to stress, iii) response to oxidative stress and iv) aging, were found in the up-regulated genes of turbot suggesting a still evidenced remarkable immune response at 72h *post*-injury. The down-regulated genes in turbot denote functions relatively to: i) skeletal system development, ii) collagen fibril organization, iii) extracellular matrix organization, iv) ossification, v) bone development and vi) extracellular structure organization. These represented functions shows that inhibition in the skin and skeletal development and organization is observed, indicating that the animals were repartitioning their regeneration machinery away from supposedly enhanced functions towards immune response (Tables 4.3, 4.5, 4.7 and 4.8; annex 6). In brill, functions related to i) cellular division and ii) cell cycle were identified in the up-regulated genes. In the other hand, vasculature development and morphogenesis were the functions evidenced in the down-regulated genes. These results suggest, once again, the repartitioning of some functions (e. g., muscle development) away from normal housekeeping functions towards epithelial regeneration (Tables 4.3, 4.5, 4.7 and 4.8; annex 6). The functions which diverged in their expression between species were i) muscle cell proliferation, ii) collagen fibril organization, iii) cell cycle and iv) cell division. These results suggest differences in the skin repair, regeneration and organization between turbot and brill, as can be observed in the Tables 4.4 and 4.6-4.8 (annex 6). However, one aspect to bear in mind is that the analysis was focused only on the most DE genes with a putative function assigned, which limits the overall analysis and, therefore, the pathways invoked could only be inferred from those genes with a known functional annotation. The unknown genes and those which were not included in

this analysis will form an important aspect of future investigations, particularly those that are DE in each and between species. Moreover, as demonstrated by Vieira et al. (2011), the skin and scales regeneration is a dramatic process which shows a major manifestation within the first three days after the injury. This fact turns the understanding procedure into a posterior required acquirement of a more detailed and time coursed experiment.

Table 4.7. Significantly DE expressed relevant genes within and between species, respectively.

Accession number	Probe Name	Gene description	Putative function	Mean Log_2 ratio	P value
Turbot					
BAF62126	R4_58772.1	Tumor necrosis factor receptor superfamily, member 6b, decoy	Apoptotic programmed cell death: Protects against apoptosis.	5,316	0,004
BAJ10976	R4_9416	Serpin peptidase inhibitor, clade E (nexin, plasminogen activator inhibitor type 1), member 1	Blood coagulation. Circadian rhythm. Extracellular matrix organization. Fibrinolysis. Gene expression.	3,107	0,004
ABX57795	R4_3601	Growth hormone-releasing hormone receptor second type	Signal transduction. Cell surface receptor signaling pathway. G-protein coupled receptor signaling pathway.	2,998	0,035
IPI00473066	R4_62250	Mannose receptor, C type 1b	Receptor-mediated endocytosis.	1,732	0,021
BAC65225	R4_26533.1	Tumor necrosis factor receptor-1	Cell surface receptor signaling pathway. Death-inducing signaling complex assembly. Tumor necrosis factor-mediated signaling pathway.	1,534	0,070
NP_998231	R4_32855	Hexokinase 2	Canonical glycolysis. Carbohydrate metabolic process. Glucose metabolic process. Glucose transport. Transmembrane transport.	1,639	0,045
ABH06553	R4_14311.1	Proto-oncogene protein c-Fos	DNA methylation. Fc-epsilon receptor signaling pathway. Inflammatory response. Innate immune response.	0,520	0,651
NP_001122290	R4_48682r.2	Tumor necrosis factor ligand superfamily member 18	Cell-cell signaling. Negative regulation of apoptotic process. Signal transduction.	-0,575	0,001
Brill					
AGA84100	R4_11184	Vascular endothelial growth factor A	Blood coagulation. Nervous system development. Platelet activation and degranulation. Positive regulation of leukocyte migration. Vasculogenesis.	-1,498	0,036
NP_001230143	R4_13876r	p90 ribosomal S6 kinase	Axon guidance. Central nervous system development. Signal transduction. Synaptic transmission.	1,635	0,003
ABH06553	R4_14311.1	Proto-oncogene protein c-Fos	DNA methylation. Fc-epsilon receptor signaling pathway. Inflammatory response. Innate immune response.	1,951	0,006
BAJ10976	R4_9416	Serpin peptidase inhibitor, clade E (nexin, plasminogen activator inhibitor type 1), member 1	Blood coagulation. Circadian rhythm. Extracellular matrix organization. Fibrinolysis. Gene expression.	3,722	0,013
Between species					
Accession number	**Probe Name**	**Gene description**	**Putative function**	**Mean Log_2 ratio (brill)**	**Mean Log_2 ratio (turbot)**	**Mean Log_2 ratio dif**	**P value**

NP_001230143	R4_13876r	p90 ribosomal S6 kinase	Axon guidance. Central nervous system development. Signal transduction. Synaptic transmission.	1,635	-0,266	1,901	0,001
AGA84100	R4_11184	Vascular endothelial growth factor A	Blood coagulation. Nervous system development. Platelet activation and degranulation. Positive regulation of leukocyte migration. Vasculogenesis.	-1,498	0,953	-2,452	0,011
ABX57795	R4_3601	Growth hormone-releasing hormone receptor second type	Signal transduction. Cell surface receptor signaling pathway. G-protein coupled receptor signaling pathway.	0,043	2,998	-2,955	0,038
NP_001017756	R4_19830	GRB2-related adaptor protein 2a	T cell costimulation. T cell receptor signaling pathway. Cell-cell signaling. Innate immune response. Positive regulation of signal transduction.	1,205	-0,892	2,097	0,008

Table 4.8.Expressed and differently expressed genes from the Fibroblast Growth Factor signaling Pathway and the Ectodysplasin Pathway in each and between species, respectively..

Probe Name	**Description**	**Putative function**	**Mean Log_2 ratio**	**P value**
		Turbot		
R4_9919.2	Mitogen-activated protein kinase 9 isoform JNK2 alpha2-like	Innate immune response. Regulation of sequence-specific DNA binding transcription factor activity. Response to stress. Stress-activated MAPK cascade.	0,514	0,080
R4_3080	Bisphosphate nucleotidase 1	Dephosphorylation. Nervous system development. Nucleobase-containing compound metabolic process. Xenobiotic metabolic process.	0,080	0,743
R4_25837	Mitogen-activated protein kinase 8B-like	Apoptotic process. Apoptotic signaling pathway. Innate immune response. Positive regulation of apoptotic process. Response to stress.	-0,390	0,145
		Brill		
R4_25778r.2	Fibroblast growth factor 8 b	Epidermal growth factor receptor signaling pathway. Innate immune response. Insulin receptor signaling pathway.	-0,497	0,186
R4_9919.2	Mitogen-activated protein kinase 9 isoform JNK2 alpha2-like	Innate immune response. Regulation of sequence-specific DNA binding transcription factor activity. Response to stress. Stress-activated MAPK cascade.	-1,973	0,043

Between species

Probe Name	**Description**	**Putative function**	**Mean Log_2 ratio (brill)**	**Mean Log_2 ratio (turbot)**	**Mean Log_2 ratio dif**	**P value**
R4_9919.2	Mitogen-activated protein kinase 9 isoform JNK2 alpha2-like	Innate immune response. Regulation of sequence-specific DNA binding transcription factor activity. Response to stress. Stress-activated MAPK cascade.	-1,973	0,514	-2,487	0,031

4.3. Microarray validation by RT-PCR

Nine genes (including housekeeping) were used to validate the turbot microarray and 6 for the brill microarray data. Spearman correlation showed a high and significant correspondence between both data sets (microarray vs RT-PCR). Although the number of genes used is not too high, results suggest the consistency of microarray data (Morey et al. 2006; Robledo et al. 2014). Both data sets were represented in a plot diagram including the regression line to visualize their correspondence (Figures 4.4 and 4.5).

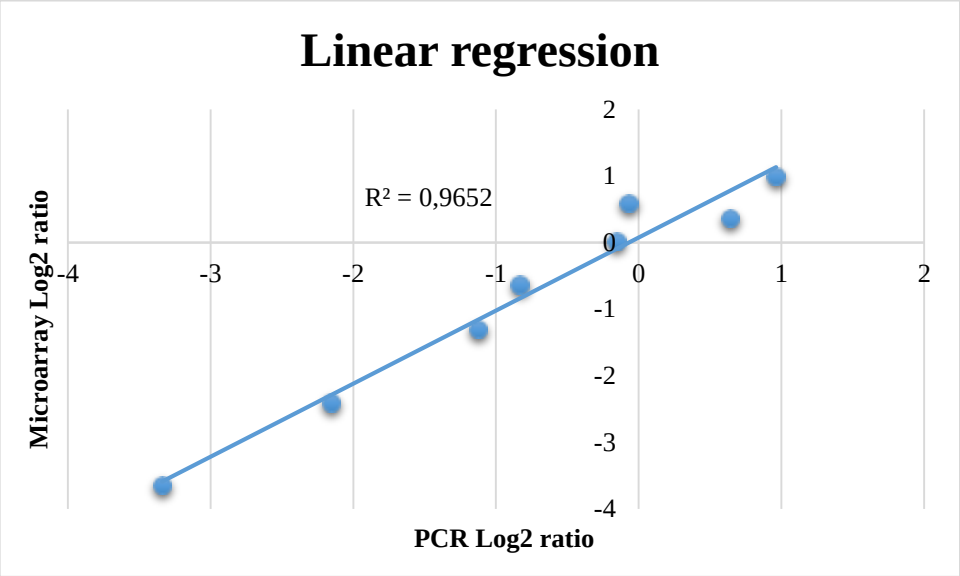

Figure 4.4. Representation of the linear regression and respective coefficient (r^2) between the data results of the microarray and the RT-PCR for turbot.

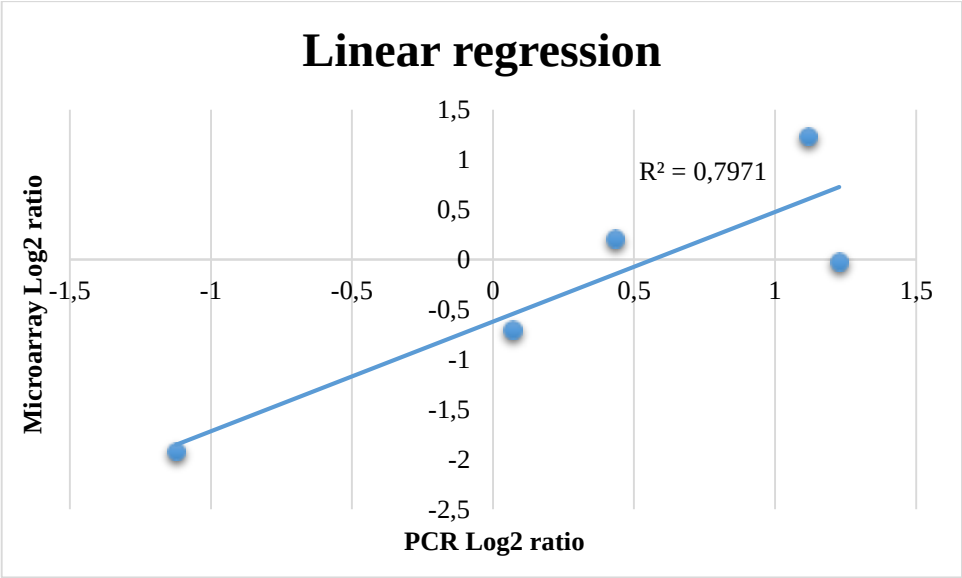

Figure 4.5. Representation of the linear regression and respective coefficient (r^2) between the data results of the microarray and the RT-PCR for brill.

5. CONCLUSIONS

The fish skin is a very complex organ, since it interferes with various essential functions. Loss of scales and/ or superficial injuries may occur in both wild and cultivated species and, as a very important organ, must be re-established as soon as possible. There are scarce molecular and histological studies of the fish skin and scales regeneration (Faílde et al. 2014; Vieira et al. 2011; Mittal & Munshi 1974; Quilhac & Sire 1999; Rakers et al. 2010) but no molecular study was done before in turbot and brill skin regeneration. This study confirms the genetic proximity between both species and shows genetic differences in skin regeneration between them that are likely related to their different skin structure. This is a preliminary work and more detailed and elaborate studies of the skins response to injury between these two congeneric species should be carried out in the future. Furthermore, this work may serve as a basis for studies with potential use in aquaculture of both species.

6. REFERENCES

Agilent Technologies, 2014. *One-Color Microarray-Based Gene Low Input Quick Amp Labeling Protocol*, Agilent Technologies.

Alvarez-Pellitero, P., 2008. Fish immunity and parasite infections: from innate immunity to immunoprophylactic prospects. *Veterinary immunology and immunopathology*, 126(3-4), pp.171–98.

Anderson, C.D. & Roberts, R.J., 1975. A comparison of the effects of temperature on wound healing in a tropical and a temperate teleost. *Journal of Fish Biology*, 7(2), pp.173–182.

Azevedo, M. et al., 2008. Phylogenetic analysis of the order *Pleuronectiformes* (*Teleostei*) based on sequences of 12S and 16S mitochondrial genes. *Genetics and Molecular Biology.*, 31, pp.284–292.

Benjamin, M., 1988. Mucochondroid (mucous connective) tissues in the heads of teleosts. *Anatomy and embryology*, 178(5), pp.461–74.

Besyst, B., Cattrijsse, A. & Mees, J., 1999. Feeding ecology of juvenile flatfishes of the surf zone of a sandy beach. *Journal of Fish Biology*, 55, pp.1171–1186.

Blanquer, A. et al., 1992. Allozyme variation in turbot (*Psetta maxima*) and brill (*Scophthalmus rhombus*) (*Osteichthyes, Pleuronectiformes, Scophthalmidae*) throughout their range in Europe. *Journal of Fish Biology.*, 41, pp.725–736.

Bouza, C. et al., 2002. Allozyme and microsatellite diversity in natural and domestic populations of turbot (*Scophthalmus maximus*) in comparison with other *Pleuronectiformes*. *Canadian Journal of Fisheries and Aquatic Sciences*, 59(9), pp.1460–1473.

Brown, G.A. & Wellings, S.R., 1969. Collagen formation and calcification in teleost scales. *Zeitschrift für Zellforschung und mikroskopische Anatomie (Vienna, Austria : 1948)*, 93(4), pp.571–82.

Bullock, A.M. & Roberts, R.J., 1980. Inhibition of epidermal migration in the skin of rainbow trout *Salmo gairdneri Richardson*, in the presence of achronogemic *Aeromonas salmonicida*. *Journal of Fish Diseases*, 3, pp.517–24.

Bullock, A.M. & Roberts, R.J., 1974. The dermatology of marine teleost fish. I. The normal integument. *Oceanography and marine biology - an annual review*, 13, pp.383–411.

Campinho, M.A. et al., 2007. Molecular, cellular and histological changes in skin from a larval to an adult phenotype during bony fish metamorphosis. *Cell and tissue research*, 327(2), pp.267–84.

Casas, L. et al., 2013. Disappearing Scales in Carps: Re-Visiting Kirpichnikov's Model on the Genetics of Scale Pattern Formation. *PLoS ONE*, 8(12).

Colosimo, P.F. et al., 2005. Widespread parallel evolution in sticklebacks by repeated fixation of Ectodysplasin alleles. *Science (New York, N.Y.)*, 307(5717), pp.1928–33.

Craig, A.S., Eikenberry, E.F. & Parry, D.A., 1987. Ultrastructural organization of skin: classification on the basis of mechanical role. *Connective tissue research*, 16(3), pp.213–23.

Daniels, H. V. & Watanabe, W.O., 2010. *Practical Flatfish Culture and Stock Enhancement*, Wiley-Blackwell.

Denton, E.J. & Nicol, J.A.C., 2009. A survey of reflectivity in silvery teleosts. *Journal of the Marine Biological Association of the United Kingdom*, 46(03), p.685.

Faílde, L.D. et al., 2014. Morphological, immunohistochemical and ultrastructural characterization of the skin of turbot (*Psetta maxima L.*). *Tissue & cell*, 46(5), pp.334–42.

FAO, 2015. Fisheries and aquaculture software. FishStatJ - software for fishery statistical time series. Available at: http://www.fao.org/fishery/statistics/software/fishstatj/en.

Ferguson, H.W., 2006. *Systemic Pathology of Fish: A Text and Atlas of Normal Tissues in Teleosts and Their Responses in Disease* 2 nd ed. H. W. Ferguson, ed., London: Scotian Press.

Froese, R. & Pauly, D., 2015. FishBase. *World Wide Web electronic publication.* Available at: http://www.fishbase.org/.

Goldsmith, L.A., 1991. *Physiology, biochemistry, and molecular biology of the skin* 2nd ed. L. A. Goldsmith, ed., New York: Oxford University Press.

Groff, J.M., 2001. Cutaneous biology and diseases of fish. *The veterinary clinics of North America. Exotic animal practice*, 4(2), pp.321–411, v–vi.

Van der Hammen, T. et al., 2013. Population ecology of turbot and brill: What can we learn from two rare flatfish species? *Journal of Sea Research*, 84, pp.96–108.

Harder, W., 1976. *Anatomy of fishes* T. . S. Sokoloff, ed., Stuttgart, Germany: Schweizerbart Science Publishers.

Harris, M.P., 2012. Comparative genetics of postembryonic development as a means to understand evolutionary change. *Journal of Applied Ichthyology*, 28(3), pp.306–315.

Harris, M.P. et al., 2008. Zebrafish *eda* and *edar* mutants reveal conserved and ancestral roles of ectodysplasin signaling in vertebrates. *PLoS genetics*, 4(10).

Huang, D.W., Sherman, B.T. & Lempicki, R.A., 2009a. Bioinformatics enrichment tools: paths toward the comprehensive functional analysis of large gene lists. *Nucleic acids research*, 37(1), pp.1–13.

Huang, D.W., Sherman, B.T. & Lempicki, R.A., 2009b. Systematic and integrative analysis of large gene lists using DAVID bioinformatics resources. *Nature protocols*, 4(1), pp.44–57.

Kobayashi, S. et al., 1972. Calcification and nucleation in fish-scales. H. K. Erban, ed. *Biomineralization Research Reports.*, 6, pp.84–90.

Kondo, S. et al., 2001. The medaka *rs-3* locus required for scale development encodes ectodysplasin-A receptor. *Current biology : CB*, 11(15), pp.1202–6.

Lagler, K.E., Bardach, J.E. & Miller, R.R., 1962. Ichthylogy. *Journal of the Marine Biological Association of the United Kingdom*, 43(02), p.571.

Lanzing, W.J. & Wright, R.G., 1976. The ultrastructure and calcification of the scales of *Tilapia mossambica* (Peters). *Cell and tissue research*, 167(1), pp.37–47.

Liu, L. et al., 2013. Short-term feed deprivation alters immune status of surface mucosa in channel catfish (*Ictalurus punctatus*). *PloS one*, 8(9).

Long, J.H. et al., 1996. Functions of fish skin: Flexural stiffness and steady swimming of longnose gar *Lepisosteus osseus*. *Journal of Experimental Biology*, 199(10), pp.2139–2151.

Long, Y. et al., 2013. *De novo* assembly of mud loach (*Misgurnus anguillicaudatus*) skin transcriptome to identify putative genes involved in immunity and epidermal mucus secretion. *PloS one*, 8(2).

Micallef, G. et al., 2012. Exploring the transcriptome of Atlantic salmon (*Salmo salar*) skin, a major defense organ. *Marine biotechnology (New York, N.Y.)*, 14(5), pp.559–69.

Mikkola, M.L. & Thesleff, I., 2003. Ectodysplasin signaling in development. *Cytokine & growth factor reviews*, 14(3-4), pp.211–24.

Millán, A. et al., 2010. Design and performance of a turbot (*Scophthalmus maximus*) oligo-microarray based on ESTs from immune tissues. *Marine biotechnology (New York, N.Y.)*, 12(4), pp.452–65.

Millán, A. et al., 2011. Gene expression profiles of the spleen, liver, and head kidney in turbot (*Scophthalmus maximus*) along the infection process with *Aeromonas salmonicida* using an immune-enriched oligo-microarray. *Marine biotechnology (New York, N.Y.)*, 13(6), pp.1099–114.

Mittal, A.K. et al., 1976. Lipids in the skin of a catfish *Heteropneustes fossilis* (Bloch) (*Heteropneustidae, Pisces*). A histochemical investigation. *Histochemistry*, 48(3), pp.177–185.

Mittal, A.K. & Munshi, J.S., 1974. On the regeneration and repair of superficial wounds in the skin of *Rita rita* (Ham.) (*Bagridae, Pisces*). *Acta anatomica*, 88(3), pp.424–42.

Mittal, A.K., Rai, A.K. & Banerjee, T.K., 1978. Studies on the pattern of healing of wounds in the skin of a catfish *Heteropneustes fossilis* (Bloch) (*Heteropneustidae, pisces*). *Z Mikrosk Anat Forsch*, 91, pp.270–286.

Morey, J.S., Ryan, J.C. & Van Dolah, F.M., 2006. Microarray validation: factors influencing correlation between oligonucleotide microarrays and real-time PCR. *Biological procedures online*, 8, pp.175–93.

Moyle, P.B. & Cech, J.J.J., 1988. *Fishes: An Introduction to Ichthyology*. 2 ed., Englewood Cliffs, New Jersey: Prentice Hall.

Muus, B.J. & Nielsen, J.G., 1999. Sea fish. In *Scandinavian Fishing Year Book*. Hedehusene, Denmark, p. 340.

Pardo, B.G. et al., 2012. Gene expression profiles of spleen, liver, and head kidney in turbot (*Scophthalmus maximus*) along the infection process with *Philasterides dicentrarchi* using an immune-enriched oligo-microarray. *Marine biotechnology (New York, N.Y.)*, 14(5), pp.570–82.

Pardo, B.G. et al., 2001. Localization of ribosomal genes in *Pleuronectiformes* using *Ag-*, *CMA3*-banding and *in situ* hybridization. *Heredity*, 86(5), pp.531–536.

Pardo, B.G. et al., 2005a. New microsatellite markers in turbot (*Scophthalmus maximus*) derived from an enriched genomic library and sequence databases. *Molecular Ecology Notes*, 5(1), pp.62–64.

Pardo, B.G. et al., 2005b. Phylogenetic analysis of flatfish (Order Pleuronectiformes) based on mitochondrial 16s rDNA sequences. *Scientia Marina*, 69(4), pp.531–543.

Pereiro, P. et al., 2012. High-throughput sequence analysis of turbot (*Scophthalmus maximus*) transcriptome using 454-pyrosequencing for the discovery of antiviral immune genes. *PloS one*, 7(5).

Pierce, A.L. et al., 2007. Prolactin receptor, growth hormone receptor, and putative somatolactin receptor in Mozambique tilapia: tissue specific expression and differential regulation by salinity and fasting. *General and comparative endocrinology*, 154(1-3), pp.31–40.

Proksch, E., Brandner, J.M. & Jensen, J.-M., 2008. The skin: an indispensable barrier. *Experimental Dermatology*, 17(12), pp.1063–1072.

Quilhac, A. & Sire, J.Y., 1999. Spreading, proliferation, and differentiation of the epidermis after wounding a cichlid fish, *Hemichromis bimaculatus*. *The Anatomical record*, 254(3), pp.435–51.

Rakers, S. et al., 2010. 'Fish matters': the relevance of fish skin biology to investigative dermatology. *Experimental dermatology*, 19(4), pp.313–24.

Ribas, L. et al., 2013. A combined strategy involving Sanger and 454 pyrosequencing increases genomic resources to aid in the management of reproduction, disease control and genetic selection in the turbot (*Scophthalmus maximus*). *BMC genomics*, 14(1), p.180.

Roberts, R.J., 2012. *Fish Pathology* 4th ed. J. W. & Sons, ed., Wiley-Blackwell.

Roberts, R.J., 1975. The effect of temperature on diseases and their histopathological manifestations in fish. In W. E. Ribelin & G. Migaki, eds. *The pathology of fishes.* Madison: University of Wisconsin, pp. 477–496.

Roberts, R.J. & Bullock, A.M., 1976. The dermatology of marine teleost fish. II. Dermatopathology of the integument. *Oceanography and Marine Biology: An Annual Review*.

Robledo, D. et al., 2014. Analysis of qPCR reference gene stability determination methods and a practical approach for efficiency calculation on a turbot (*Scophthalmus maximus*) gonad dataset. *BMC Genomics*, 15(1), p.648.

Rodríguez Villanueva, J.L. & Fernández Souto, B., 2009. *Scophthalmus maximus*. *Cultured aquatic species fact sheets*. Available at: http://www.fao.org/fishery/culturedspecies/Psetta_maxima/en.

Rohner, N. et al., 2009. Duplication of *fgfr1* permits *Fgf* signaling to serve as a target for selection during domestication. *Current biology : CB*, 19(19), pp.1642–7.

Schönbörner, A.A., Boivin, G. & Baud, C.A., 1979. The mineralization processes in Teleost fish scales. *Cell and Tissue Research*, 202(2).

Schroeder, A. et al., 2006. The RIN: an RNA integrity number for assigning integrity values to RNA measurements. *BMC molecular biology*, 7(1), p.3.

Sire, J.-Y. et al., 1997. Scale development in zebrafish (*Danio rerio*). *Journal of Anatomy*, 190(4), pp.545–561.

Sire, J.-Y. & Géraudie, J., 1984. Fine structure of regenerating scales and their associated cells in the cichlid *Hemichromis bimaculatus* (Gill). *Cell and Tissue Research*, 237(3).

Speare, D.J. & Mirailimi, S.M., 1992. Pathology of the mucous coat of trout skin during an erosive bacterial dermatitis. *Journal of Comparative Pathology*, 106, pp.210–11.

Universidade do Algarve, 2013. ENGENHARIA BIOLÓGICA - Apresentação. *Universidade do Algarve webpage*, p.1. Available at: http://www.ualg.pt/pt/curso/1458.

Vieira, F. a et al., 2011. Skin healing and scale regeneration in fed and unfed sea bream, *Sparus auratus*. *BMC Genomics*, 12(1), p.490.

Waterman, R.E., 1970. Fine structure of scale development in the teleost, *Brachydanio rerio*. *The Anatomical record*, 168(3), pp.361–79.

Wheeler, A., 1992. A list of the common and scientific names of fishes of the British Isles. *Journal of Fish Biology.*, 41, pp.1–37.

Whitear, M., 1977. A functional comparison between the epidermis of fish and of amphibians. *Symposia of the Zoological Society of London*, 39, pp.291–313.

Whitear, M., 2009. The skin surface of bony fishes. *Journal of Zoology*, 160(4), pp.437–454.

Zylberberg, L. et al., 2003. Structural Peculiarities of the Tubercles in the Skin of the Turbot, *Scophthalmus maximus* (L., 1758) (Osteichthyes, Pleuronectiformes, Scophthalmidae). *Journal of Morphology*, 258(1), pp.84–96.

Zylberberg, L. & Nicolas, G., 1982. Ultrastructure of scales in a teleost (*Carassius auratus L.*) after use of rapid freeze-fixation and freeze-substitution. *Cell and Tissue Research*, 223(2), pp.349–367.

7. ANNEXES

7.1. Annex 1

The list of 1564 skin-related genes is provided in digital format as an excel file and contains only their respective accession numbers.

7.2. Annex 2

Table 7.1. BLAST result from the skin-related sequences present in the DB5 against the microarray probes.

Species	Accession no	Transcript Name	Turbot 5 ID	Probe Name	% ID	e-value	alignment lenght
Danio rerio	NP_001001399	translocon-associated protein subunit beta precursor	433	R4_55735r	100.00	6E-23	56
Danio rerio	NP_001001406	cartilage-associated protein precursor	7063	R4_7300	100.00	2E-22	55
Danio rerio	NP_001001842	cellular retinoic acid binding protein 1b	13483	R4_14582r	100.00	5E-23	56
Danio rerio	NP_001001886	ubiquitin carboxyl-terminal hydrolase 25	48797	R4_31746	100.00	1E-22	55
Danio rerio	NP_001001889	catenin, beta 2	18361	R4_44031r	100.00	5E-21	53
Danio rerio	NP_001002038	annexin A6	7338	R4_7679.2	100.00	4E-22	55
Danio rerio	NP_001002058	SUMO-activating enzyme subunit 1	1349	R4_23742	100.00	3E-22	55
Danio rerio	NP_001002064	26S protease regulatory subunit 6A	10845	R4_11936.2	100.00	3E-22	55
Danio rerio	NP_001002072	ubiquitin-conjugating enzyme E2 L3	696	R4_49441	100.00	8E-23	56
Danio rerio	NP_001002131	26S proteasome non-ATPase regulatory subunit 8	7534	R4_12530	100.00	3E-22	55
Danio rerio	NP_001002158	reticulocalbin-3 precursor	19111	R4_8643	100.00	3E-22	55
Danio rerio	NP_001002181	bifunctional methylenetetrahydrofolate dehydrogenase/cyclohydrolase, mitochondrial	499	R4_49139r	100.00	3E-22	55
Danio rerio	NP_001002298	ATPase asna1	4805	R4_4703	100.00	9E-23	55
Danio rerio	NP_001002355	thimet oligopeptidase	14290	R4_15437r.1	100.00	1E-22	55
Danio rerio	NP_001002374	methylmalonate-semialdehyde dehydrogenase [acylating], mitochondrial	1823	R4_16094	100.00	9E-23	56
Danio rerio	NP_001002386	lysine--tRNA ligase	900	R4_917	100.00	4E-22	55
Danio rerio	NP_001002468	peroxiredoxin-2	9901	R4_11057r.1	100.00	9E-23	56
Danio rerio	NP_001002543	proteasome subunit beta type-10	4051	R4_3948.2	100.00	2E-22	55
Danio rerio	NP_001002548	transcription initiation factor TFIID subunit 11	1141	R4_612	100.00	2E-22	55
Danio rerio	NP_001002566	ras-related protein Rab-10	1682	R4_1622.2	100.00	2E-22	55

Annex 2

Danio rerio	NP_001002575	transmembrane and coiled-coil domains 1	35001	R4_59940r	100.00	2E-22	55
Danio rerio	NP_001002589	proteasome subunit alpha type-6	681	R4_10650r.2	100.00	2E-22	55
Danio rerio	NP_001002600	ubiquitin-conjugating enzyme E2 R2	34528	R4_20498r	100.00	1E-22	55
Danio rerio	NP_001002609	proteasome subunit beta type-2	985	R4_54607	98.15	1E-19	54
Danio rerio	NP_001002667	solute carrier family 25 member 36-A	6406	R4_6475	98.18	2E-21	55
Danio rerio	NP_001002742	trafficking protein particle complex subunit 1	10736	R4_50606	100.00	1E-22	55
Danio rerio	NP_001002749	-	49051	R4_31951	100.00	1E-22	55
Danio rerio	NP_001003427	proteasome subunit alpha type-1	668	R4_21756r.1	100.00	2E-22	55
Danio rerio	NP_001003488	pyruvate kinase isozymes M1/M2	1178	R4_1159	100.00	1E-23	58
Danio rerio	NP_001003546	GINS complex subunit 4	35043	R4_1326r	100.00	3E-22	55
Danio rerio	NP_001003570	-	10859	R4_11952r	100.00	1E-22	55
Danio rerio	NP_001003727	kelch-like protein 31	9445	R4_10636	100.00	3E-22	55
Danio rerio	NP_001003832	26S protease regulatory subunit S10B	587	R4_11104	100.00	3E-22	55
Danio rerio	NP_001003834	DNA topoisomerase 2-alpha	60248	R4_9084r	100.00	9E-23	55
Danio rerio	NP_001003860	protein BUD31 homolog	4108	R4_4003	100.00	2E-22	55
Danio rerio	NP_001003875	U1 small nuclear ribonucleoprotein 70 kDa	39137	R4_24049r	100.00	1E-22	55
Danio rerio	NP_001003882	seryl-tRNA synthetase, cytoplasmic	9388	R4_10577r	100.00	1E-22	56
Danio rerio	NP_001004289	splicing factor 3A subunit 3	12366	R4_26618r	100.00	5E-24	58
Danio rerio	NP_001004575	phosphofructokinase, muscle a	12970	R4_14061	100.00	7E-23	56
Danio rerio	NP_001004578	EH domain-containing protein 1	80950	R4_58237	100.00	8E-23	55
Danio rerio	NP_001004583	solute carrier family 35 member B1	10121	R4_11258r	100.00	7E-23	56
Danio rerio	NP_001004586	histidyl-tRNA synthetase, cytoplasmic	33583	R4_20072r	100.00	1E-22	55
Danio rerio	NP_001004603	argininosuccinate synthase	1019	R4_16556	100.00	3E-22	55
Danio rerio	NP_001005590	serine/threonine-protein phosphatase 2A 65 kDa regulatory subunit A beta isoform	1269	R4_1245	100.00	6E-22	55
Danio rerio	NP_001005947	ADP-ribosylation factor-like protein 2	1922	R4_1850	100.00	2E-22	55
Danio rerio	NP_001006000	nuclear transport factor 2	50154	R4_32867	100.00	8E-23	55

Annex 2

Danio rerio	NP_001006035	PEST proteolytic signal-containing nuclear protein	9435	R4_10624r	100.00	1E-22	56
Danio rerio	NP_001006073	angiopoietin-related protein 7 precursor	12852	R4_13940	100.00	3E-22	55
Danio rerio	NP_001006077	exosome complex exonuclease RRP45	49891	R4_32651	98.18	9E-22	55
Danio rerio	NP_001006098	3-hydroxyacyl-CoA dehydrogenase type-2	36247	R4_21907r.1	100.00	2E-22	55
Danio rerio	NP_001007056	ras-related protein Rap-2c	2155	R4_2074.1	100.00	3E-22	55
Danio rerio	NP_001007162	ras-related protein Rab-1A	15823	R4_17172.1	100.00	2E-22	55
Danio rerio	NP_001007384	-	7536	R4_57616r	100.00	1E-22	55
Danio rerio	NP_001007767	stress-induced-phosphoprotein 1	907	R4_46581r	100.00	5E-22	55
Danio rerio	NP_001007769	phenylalanyl-tRNA synthetase beta chain	2473	R4_53305	100.00	4E-22	55
Danio rerio	NP_001007775	pre-mRNA-splicing factor SPF27	1495	R4_21560r	100.00	3E-22	55
Danio rerio	NP_001007778	eukaryotic translation initiation factor 4E	582	R4_643	100.00	3E-22	55
Danio rerio	NP_001009898	cyclin-dependent kinase 2-associated protein 2	970	R4_978	100.00	6E-23	56
Danio rerio	NP_001009902	peptidyl-prolyl cis-trans isomerase H isoform 1	612	R4_10849r	100.00	2E-22	55
Danio rerio	NP_001012498	betaine--homocysteine S-methyltransferase 1	9262	R4_10464	100.00	3E-22	55
Danio rerio	NP_001012499	anterior gradient protein 2 homolog precursor	9202	R4_10404	100.00	1E-22	55
Danio rerio	NP_001012501	cellular retinoic acid binding protein 2, b	11960	R4_13032	98.18	3E-20	55
Danio rerio	NP_001013311	chromatin accessibility complex protein 1	731	R4_772	100.00	2E-22	55
Danio rerio	NP_001013344	replication factor C subunit 2	7630	R4_33555.2	100.00	2E-22	55
Danio rerio	NP_001013363	RNA-binding protein 8A	4333	R4_4212	100.00	2E-22	55
Danio rerio	NP_001013465	speckle-type POZ protein-like A	25429	R4_22727r	96.36	1E-18	55
Danio rerio	NP_001013587	-	76418	R4_14654r	100.00	3E-22	55
Danio rerio	NP_001014311	eukaryotic translation initiation factor 4, gamma 2a	52295	R4_34693	100.00	1E-22	55
Danio rerio	NP_001014324	low molecular weight phosphotyrosine protein phosphatase isoform 1	35140	R4_12996	100.00	1E-22	55
Danio rerio	NP_001014367	cystathionine-beta-synthase b	9189	R4_10390r	98.18	2E-20	55
Danio rerio	NP_001017557	-	37891	R4_23120.2	100.00	2E-22	55

Annex 2

Danio rerio	NP_001017574	cell division cycle-associated protein 7	1627	R4_11656r	100.00	3E-22	55
Danio rerio	NP_001017582	small nuclear ribonucleoprotein Sm D2	708	R4_745	100.00	2E-22	55
Danio rerio	NP_001017585	exosome complex exonuclease RRP42	1163	R4_12913r	100.00	1E-23	57
Danio rerio	NP_001017639	deoxycytidylate deaminase	1201	R4_39141.1	100.00	4E-22	55
Danio rerio	NP_001017640	alcohol dehydrogenase [NADP(+)] B	6478	R4_6562.2	100.00	2E-22	55
Danio rerio	NP_001017654	-	15164	R4_16455	98.18	2E-20	55
Danio rerio	NP_001017688	probable aminopeptidase NPEPL1	10349	R4_11470	100.00	4E-22	55
Danio rerio	NP_001017690	U11/U12 small nuclear ribonucleoprotein 25 kDa protein	2490	R4_2400	100.00	2E-22	55
Danio rerio	NP_001017700	protein mago nashi homolog	2782	R4_10949r	100.00	2E-21	54
Danio rerio	NP_001017768	COP9 signalosome complex subunit 6	522	R4_2066r	100.00	2E-22	55
Danio rerio	NP_001017801	proteasome subunit beta type-4	1759	R4_1697r.1	100.00	2E-22	55
Danio rerio	NP_001017880	NADH dehydrogenase [ubiquinone] 1 beta subcomplex subunit 9	32980	R4_19733	100.00	1E-22	55
Danio rerio	NP_001018337	glutathione peroxidase 7 precursor	1122	R4_1116	100.00	2E-22	55
Danio rerio	NP_001018355	urea transporter 2	77693	R4_55457	100.00	2E-22	55
Danio rerio	NP_001018441	transcription initiation factor IIA subunit 2	35111	R4_67167	100.00	2E-22	55
Danio rerio	NP_001018448	-	76041	R4_54111	100.00	9E-23	55
Danio rerio	NP_001018464	glycogen phosphorylase, muscle form	257	R4_324r	100.00	1E-22	55
Danio rerio	NP_001018587	-	40817	R4_25331r.1	100.00	1E-22	55
Danio rerio	NP_001018589	prolyl endopeptidase	2593	R4_2503r.2	100.00	4E-22	55
Danio rerio	NP_001019625	N-ethylmaleimide-sensitive factor b	51591	R4_34090r.2	100.00	1E-22	55
Danio rerio	NP_001020354	slow skeletal ventricular myosin alkali light chain 3	72746	R4_3355	100.00	5E-23	56
Danio rerio	NP_001020705	alpha globin regulatory element containing-like	6934	R4_7145	98.18	5E-21	55
Danio rerio	NP_001025256	-	14583	R4_15761r	98.18	5E-21	55
Danio rerio	NP_001025448	-	75592	R4_53760	100.00	2E-22	55
Danio rerio	NP_001025456	villin 2	9266	R4_20830	100.00	7E-22	55
Danio rerio	NP_001028278	protein cornichon homolog	857	R4_41076	100.00	5E-22	55

Annex 2

Danio rerio	NP_001028279	dyskerin	739	R4_20737	100.00	1E-22	56
Danio rerio	NP_001028280	transmembrane emp24 domain-containing protein 9 precursor	6945	R4_7985r	100.00	5E-22	55
Danio rerio	NP_001028913	signal recognition particle 14 kDa protein	525	R4_595r	100.00	3E-22	55
Danio rerio	NP_001029350	peptidyl-prolyl cis-trans isomerase-like 1	1012	R4_1018	100.00	1E-22	55
Danio rerio	NP_001030155	cytoplasmic aconitate hydratase	10041	R4_3902	100.00	4E-22	55
Danio rerio	NP_001032454	6-phosphofructo-2-kinase/fructose-2,6-biphosphatase 4	9529	R4_10715	100.00	7E-24	58
Danio rerio	NP_001032461	-	10834	R4_9324	100.00	6E-23	56
Danio rerio	NP_001032470	-	49775	R4_32555	100.00	1E-22	55
Danio rerio	NP_001032479	ubiquitin-conjugating enzyme E2 variant 1	49190	R4_7874	100.00	8E-23	55
Danio rerio	NP_001032756	cytoskeleton-associated protein 5	61834	R4_42722r	100.00	1E-22	55
Danio rerio	NP_001032780	ubiquitin-conjugating enzyme E2 C	8663	R4_9715	100.00	2E-22	55
Danio rerio	NP_001035072	enhancer of zeste 1	2029	R4_51506	98.21	4E-21	56
Danio rerio	NP_001035389	UDP-glucose 4-epimerase	6444	R4_6523	100.00	8E-23	56
Danio rerio	NP_001035465	stathmin 1a	797	R4_50579	100.00	3E-22	55
Danio rerio	NP_001036788	histone 2A family member ZA	35120	R4_21044	100.00	2E-22	55
Danio rerio	NP_001038436	-	41455	R4_6145.1	100.00	1E-22	55
Danio rerio	NP_001038458	cysteine desulfurase, mitochondrial	1958	R4_13617r	100.00	8E-23	56
Danio rerio	NP_001038499	histone acetyltransferase KAT2B	2659	R4_2568	100.00	1E-22	56
Danio rerio	NP_001038760	phenylalanine--tRNA ligase alpha subunit	1001	R4_1004.2	100.00	2E-22	55
Danio rerio	NP_001038827	keratinocyte-associated protein 2	657	R4_709	100.00	2E-22	55
Danio rerio	NP_001038912	small CTD phosphatase 3-like	8022	R4_8721	100.00	3E-22	55
Danio rerio	NP_001039029	proteasome subunit beta type-7	558	R4_20647	100.00	2E-22	55
Danio rerio	NP_001070023	interferon-related developmental regulator 1	10038	R4_11186r	100.00	4E-22	55
Danio rerio	NP_001070026	transcription factor BTF3	9137	R4_3257	98.18	3E-21	55
Danio rerio	NP_001070097	mesencephalic astrocyte-derived neurotrophic factor precursor	9968	R4_11114	100.00	6E-22	55
Danio rerio	NP_001073498	arrestin domain-containing protein 3	18644	R4_69512.1	98.15	1E-19	54

Annex 2

Danio rerio	NP_001074122	2-oxoisovalerate dehydrogenase subunit beta, mitochondrial	1493	R4_1448	98.18	5E-20	55
Danio rerio	NP_001074139	heparan sulfate 2-O-sulfotransferase 1	2930	R4_2834r	100.00	2E-23	57
Danio rerio	NP_001075098	SWI/SNF-related matrix-associated actin-dependent regulator of chromatin subfamily A member 5	38296	R4_23410r	100.00	1E-22	55
Danio rerio	NP_001076267	14-3-3 protein beta/alpha-A	90406	R4_66975r	100.00	5E-22	55
Danio rerio	NP_001077042	26S proteasome non-ATPase regulatory subunit 14	732	R4_773.2	100.00	3E-22	55
Danio rerio	NP_001077296	collagen alpha-1(X) chain precursor	9218	R4_10415	100.00	8E-23	56
Danio rerio	NP_001077313	collagen alpha-1(XI) chain	74287	R4_52757	100.00	2E-22	55
Danio rerio	NP_001082983	ATP-dependent metalloprotease YME1L1	9526	R4_10713	100.00	3E-22	55
Danio rerio	NP_001083031	ras-related protein Rab-8A	6150	R4_6191.1	100.00	2E-22	56
Danio rerio	NP_001092721	high-mobility group box 1b	10278	R4_11398.1	100.00	4E-22	55
Danio rerio	NP_001093459	spectrin beta chain, brain 1	1996	R4_1928r	100.00	3E-22	55
Danio rerio	NP_001093467	probable global transcription activator SNF2L1	35168	R4_13802r	100.00	3E-22	55
Danio rerio	NP_001098746	hydroxyacyl-Coenzyme A dehydrogenase/3-ketoacyl-Coenzyme A thiolase/enoyl-Coenzyme A hydratase, alpha subunit a	12290	R4_1360	100.00	2E-23	57
Danio rerio	NP_001103872	UDP-glucose 6-dehydrogenase	2160	R4_11422r	100.00	4E-22	55
Danio rerio	NP_001103886	troponin T3b, skeletal, fast isoform 1	9149	R4_64344r	100.00	2E-22	55
Danio rerio	NP_001104624	-	47159	R4_30393r	100.00	6E-23	55
Danio rerio	NP_001107094	-	57103	R4_38742.2	100.00	8E-23	55
Danio rerio	NP_001108199	ring finger protein 122-like	11037	R4_12123	100.00	3E-22	55
Danio rerio	NP_001116258	threonyl-tRNA synthetase, cytoplasmic isoform 1	2375	R4_2290	100.00	3E-22	55
Danio rerio	NP_001116769	charged multivesicular body protein 2b	7058	R4_62356	100.00	1E-22	55
Danio rerio	NP_001119851	-	2878	R4_2788	100.00	4E-22	55
Danio rerio	NP_001119858	sodium- and chloride-dependent taurine transporter	37102	R4_11444r	100.00	3E-23	57
Danio rerio	NP_001121727	methylenetetrahydrofolate reductase	38432	R4_23504r	100.00	3E-22	55
Danio rerio	NP_001122153	vinculin a	2656	R4_2564	100.00	2E-22	55

Annex 2

Danio rerio	NP_001123295	proteasome subunit beta type-3	534	R4_604.1	100.00	2E-22	55
Danio rerio	NP_001136246	alanine aminotransferase 2-like	9757	R4_52131r	100.00	4E-22	55
Danio rerio	NP_001139039	3'-5' exoribonuclease CSL4 homolog	8186	R4_10468	100.00	7E-22	55
Danio rerio	NP_001139254	collagen alpha-2(V) chain precursor	9846	R4_10997	100.00	3E-22	55
Danio rerio	NP_001170924	-	31118	R4_20758	100.00	8E-23	55
Danio rerio	NP_001181907	clathrin, heavy polypeptide b (Hc)	49243	R4_32110r	100.00	1E-22	55
Danio rerio	NP_001186666	protein disulfide-isomerase A3 precursor	1488	R4_1443	100.00	4E-22	55
Danio rerio	NP_001231711	low molecular weight phosphotyrosine protein phosphatase isoform 2	9949	R4_20788	100.00	1E-22	55
Danio rerio	NP_001243119	U2 small nuclear ribonucleoprotein B"	623	R4_678	100.00	2E-22	55
Danio rerio	NP_571003	nucleoside diphosphate kinase 3	1235	R4_1214	100.00	7E-23	56
Danio rerio	NP_571038	desmin a	3504	R4_3385	100.00	2E-22	55
Danio rerio	NP_571226	proteasome subunit beta type-5	3869	R4_11837r.3	100.00	8E-23	56
Danio rerio	NP_571251	-	87510	R4_64319	100.00	2E-23	56
Danio rerio	NP_571430	kinesin-like protein KIF23	38916	R4_23889r	100.00	2E-22	55
Danio rerio	NP_571451	proteasome activator complex subunit 3	466	R4_29447	100.00	3E-22	55
Danio rerio	NP_571467	proteasome subunit beta type-8	999	R4_68428.1	100.00	6E-23	56
Danio rerio	NP_571523	SWI/SNF related, matrix associated, actin dependent regulator of chromatin, subfamily b, member 1b	45562	R4_10101	100.00	1E-22	55
Danio rerio	NP_571527	ELAV (embryonic lethal, abnormal vision, Drosophila)-like 1 (Hu antigen R)	1179	R4_12301r	100.00	3E-22	55
Danio rerio	NP_571583	coatomer subunit zeta-1	4795	R4_4698	100.00	2E-22	55
Danio rerio	NP_571639	amyloid beta A4 protein precursor	393	R4_3016	100.00	1E-22	56
Danio rerio	NP_571751	proteasome beta 11 subunit	1464	R4_1415.2	100.00	2E-23	57
Danio rerio	NP_571757	-	10014	R4_11160	100.00	2E-22	55
Danio rerio	NP_571836	ATP synthase, H+ transporting, mitochondrial F0 complex, subunit c3 (subunit 9) genome duplicate b	1501	R4_21049	100.00	2E-22	55
Danio rerio	NP_658910	glucose phosphate isomerase b	6358	R4_6426	100.00	2E-22	55

Annex 2

Danio rerio	NP_694549	retinol-binding protein 2	8326	R4_9169	98.21	2E-21	56
Danio rerio	NP_705955	translocating chain-associated membrane protein 1	2081	R4_1999	100.00	3E-22	55
Danio rerio	NP_775329	brain creatine kinase b	101	R4_115.2	100.00	1E-22	55
Danio rerio	NP_775346	protein MAK16 homolog	35131	R4_21055	100.00	3E-22	55
Danio rerio	NP_775361	V-type proton ATPase subunit E 1	3142	R4_13437	100.00	3E-22	55
Danio rerio	NP_775364	DNA replication licensing factor MCM2	2682	R4_2591	100.00	2E-22	55
Danio rerio	NP_775365	-	4161	R4_4043	100.00	5E-22	55
Danio rerio	NP_775371	nascent polypeptide-associated complex subunit alpha isoform 2	1350	R4_7866r.2	100.00	3E-22	55
Danio rerio	NP_775373	PHD finger-like domain-containing protein 5A	1021	R4_7969	100.00	1E-22	55
Danio rerio	NP_775377	V-type proton ATPase subunit H	998	R4_10091r	100.00	3E-22	55
Danio rerio	NP_776196	ruvB-like 1	11241	R4_1076.1	100.00	2E-22	55
Danio rerio	NP_777285	ruvB-like 2	737	R4_778	100.00	3E-22	55
Danio rerio	NP_848523	DNA replication licensing factor MCM5	12678	R4_13773	98.18	5E-20	55
Danio rerio	NP_853634	transcription activator BRG1	3390	R4_3276	100.00	1E-22	55
Danio rerio	NP_861431	annexin A11b	9373	R4_9157.1	100.00	3E-22	55
Danio rerio	NP_878286	glutamine synthetase	1138	R4_1127.1	100.00	3E-22	55
Danio rerio	NP_878298	V-type proton ATPase subunit B, kidney isoform	11488	R4_12552r	100.00	3E-22	55
Danio rerio	NP_892013	collagen alpha-2(I) chain precursor	34701	R4_10964r	100.00	4E-21	53
Danio rerio	NP_898895	thioredoxin reductase 3	5189	R4_5108	100.00	9E-23	56
Danio rerio	NP_922916	dolichyl-diphosphooligosaccharide--protein glycosyltransferase subunit 1 precursor	74977	R4_53292	100.00	1E-22	55
Danio rerio	NP_937853	endoplasmin precursor	9328	R4_70792r	100.00	5E-22	55
Danio rerio	NP_938152	-	11942	R4_13008	100.00	3E-22	55
Danio rerio	NP_938170	pre-mRNA-processing factor 40 homolog A	1152	R4_1138	100.00	3E-22	55
Danio rerio	NP_938180	eukaryotic translation initiation factor 4A, isoform 1A	971	R4_46579r	96.43	8E-19	56
Danio rerio	NP_942099	bisphosphoglycerate mutase 1a	8524	R4_11148	100.00	2E-22	55

Annex 2

Danio rerio	NP_944590	aconitate hydratase, mitochondrial	37711	R4_28966	100.00	3E-22	55
Danio rerio	NP_944595	DNA replication licensing factor MCM4	4137	R4_10078r	100.00	6E-23	56
Danio rerio	NP_954682	-	11094	R4_8874	100.00	3E-22	55
Danio rerio	NP_954684	collagen alpha-1(I) chain precursor	9330	R4_51370r	100.00	3E-22	55
Danio rerio	NP_955862	ribosome biogenesis protein NSA2 homolog	415	R4_517	100.00	2E-22	55
Danio rerio	NP_955963	DNA-directed RNA polymerase II subunit RPB7	491	R4_50982r.1	100.00	2E-22	55
Danio rerio	NP_955973	synaptotagmin binding, cytoplasmic RNA interacting protein, like	20805	R4_27402	100.00	3E-21	53
Danio rerio	NP_955979	COP9 signalosome complex subunit 3	2740	R4_2645	100.00	4E-22	55
Danio rerio	NP_955995	selenide, water dikinase 1	1664	R4_35123r	100.00	4E-22	55
Danio rerio	NP_956002	basic leucine zipper and W2 domain-containing protein 1-A	785	R4_31462	100.00	5E-22	55
Danio rerio	NP_956013	zgc:55512	513	R4_46324r	100.00	6E-23	56
Danio rerio	NP_956028	protein slowmo homolog 2	10508	R4_2473	100.00	5E-22	55
Danio rerio	NP_956044	proteasome 26S subunit, ATPase, 4	902	R4_3465.2	100.00	3E-22	55
Danio rerio	NP_956047	calponin 3, acidic a	226	R4_269r	100.00	1E-22	55
Danio rerio	NP_956054	small nuclear ribonucleoprotein D3 polypeptide, like	5730	R4_55158r	96.36	3E-18	55
Danio rerio	NP_956058	uridine-cytidine kinase 2-B	16310	R4_17739	100.00	3E-22	55
Danio rerio	NP_956073	protein disulfide-isomerase A4 precursor	574	R4_64833	98.18	1E-19	55
Danio rerio	NP_956083	26S proteasome non-ATPase regulatory subunit 7	13029	R4_14120.1	100.00	5E-22	55
Danio rerio	NP_956144	c20orf24 homolog	15142	R4_16432r	100.00	4E-22	55
Danio rerio	NP_956152	LIM domain binding 3	5634	R4_9969	100.00	8E-22	54
Danio rerio	NP_956159	cell division control protein 42 homolog	922	R4_936.1	100.00	3E-22	55
Danio rerio	NP_956165	S-adenosylmethionine synthase isoform type-1	806	R4_838	98.18	2E-20	55
Danio rerio	NP_956182	-	5838	R4_5841	100.00	2E-22	55
Danio rerio	NP_956186	CAAX prenyl protease 1 homolog	5163	R4_6473	100.00	1E-22	55
Danio rerio	NP_956225	protein YIF1A	9899	R4_10278	100.00	8E-23	56

Annex 2

Danio rerio	NP_956250	ras GTPase-activating protein-binding protein 1	41000	R4_25464r	100.00	1E-22	55
Danio rerio	NP_956267	ubiquitin carboxyl-terminal hydrolase 14	8442	R4_20869r	100.00	5E-22	55
Danio rerio	NP_956287	ADP-ribosylation factor 6a	9836	R4_28996	100.00	3E-22	55
Danio rerio	NP_956312	bleomycin hydrolase	13736	R4_3154	100.00	3E-22	55
Danio rerio	NP_956332	developmentally-regulated GTP-binding protein 1	495	R4_575	100.00	3E-22	55
Danio rerio	NP_956347	translocon-associated protein subunit gamma	9331	R4_931.1	100.00	2E-22	55
Danio rerio	NP_956378	-	5405	R4_5335	98.18	5E-20	55
Danio rerio	NP_956381	thioredoxin interacting protein a	8102	R4_8840	100.00	1E-22	56
Danio rerio	NP_956398	heterogeneous nuclear ribonucleoprotein A1b	3463	R4_12857	100.00	1E-22	56
Danio rerio	NP_956417	RAB11a, member RAS oncogene family, like	622	R4_10835r	100.00	2E-23	57
Danio rerio	NP_956436	sorting and assembly machinery component 50 homolog A	2457	R4_2368r	100.00	3E-22	55
Danio rerio	NP_956511	voltage-dependent anion-selective channel protein 2-like	5871	R4_5876	100.00	4E-22	55
Danio rerio	NP_956520	ribonuclease H2 subunit A	7319	R4_7651	100.00	2E-22	55
Danio rerio	NP_956547	fizzy-related protein homolog	11142	R4_12221r	98.21	1E-20	56
Danio rerio	NP_956570	-	19394	R4_25752	100.00	2E-22	55
Danio rerio	NP_956585	26S proteasome non-ATPase regulatory subunit 6	1561	R4_12053r.2	100.00	2E-22	55
Danio rerio	NP_956609	insulin receptor substrate 2	27862	R4_32247	100.00	1E-22	55
Danio rerio	NP_956616	U5 small nuclear ribonucleoprotein 40 kDa protein	6468	R4_54635	100.00	5E-22	55
Danio rerio	NP_956638	-	56803	R4_38506	100.00	6E-23	55
Danio rerio	NP_956707	-	13055	R4_14142	100.00	3E-22	55
Danio rerio	NP_956783	GDP-mannose 4,6 dehydratase isoform 2	3314	R4_3201	100.00	2E-23	57
Danio rerio	NP_956791	mannose-1-phosphate guanyltransferase alpha-B	17318	R4_62910r	98.18	5E-20	55
Danio rerio	NP_956826	dexamethasone-induced Ras-related protein 1	37567	R4_22879.1	100.00	2E-22	55
Danio rerio	NP_956840	26S proteasome non-ATPase regulatory subunit 2	15820	R4_17166.1	100.00	3E-22	55
Danio rerio	NP_956842	-	4523	R4_4412	100.00	2E-22	55
Danio rerio	NP_956848	S-methyl-5'-thioadenosine phosphorylase	4030	R4_3931r	100.00	2E-22	55

Annex 2

Danio rerio	NP_956863	TSC22 domain family protein 3	229	R4_275r	96.36	1E-18	55
Danio rerio	NP_956866	26S proteasome non-ATPase regulatory subunit 3	16846	R4_18356.2	100.00	3E-22	55
Danio rerio	NP_956871	-	1710	R4_1652	98.18	2E-20	55
Danio rerio	NP_956873	cytochrome b-245, alpha polypeptide	9894	R4_11051	100.00	4E-22	55
Danio rerio	NP_956934	ER lumen protein retaining receptor 3	1604	R4_10076	100.00	6E-24	58
Danio rerio	NP_957010	protein Asterix	547	R4_20642	100.00	2E-22	55
Danio rerio	NP_957022	RNA polymerase II subunit A C-terminal domain phosphatase SSU72	7270	R4_12460r	100.00	3E-22	55
Danio rerio	NP_957062	l-isoaspartyl protein carboxyl methyltransferase, like	5332	R4_5261	100.00	3E-22	55
Danio rerio	NP_957117	kinesin family member 4	48212	R4_31257r	100.00	2E-22	55
Danio rerio	NP_957175	-	1742	R4_1685	100.00	4E-22	55
Danio rerio	NP_957187	AMP deaminase 1	5477	R4_17902.2	100.00	3E-22	55
Danio rerio	NP_957202	tubulin gamma-1 chain	1485	R4_1440	100.00	4E-22	55
Danio rerio	NP_957211	F-box only protein 32	41269	R4_25689	100.00	2E-22	55
Danio rerio	NP_957376	calumenin-B precursor	9756	R4_1786	100.00	4E-22	55
Danio rerio	NP_957474	glycogen [starch] synthase, muscle	7690	R4_8209	100.00	9E-23	55
Danio rerio	NP_957478	26S proteasome non-ATPase regulatory subunit 1	6010	R4_6026r.1	100.00	1E-22	55
Danio rerio	NP_958473	tyrosine--tRNA ligase, cytoplasmic	2847	R4_11416	100.00	5E-22	55
Danio rerio	NP_996771	-	41345	R4_25744r	100.00	2E-22	55
Danio rerio	NP_996983	transmembrane protein 208	9933	R4_1099	100.00	3E-22	55
Danio rerio	NP_997729	cell division control protein 2 homolog	2388	R4_2305	100.00	3E-22	55
Danio rerio	NP_997732	DNA replication licensing factor MCM3	2373	R4_2288	100.00	7E-23	56
Danio rerio	NP_997734	-	44546	R4_28269	100.00	7E-23	55
Danio rerio	NP_998223	78 kDa glucose-regulated protein precursor	4125	R4_4018	100.00	4E-22	55
Danio rerio	NP_998231	-	50141	R4_32855	100.00	3E-23	56
Danio rerio	NP_998274	UMP-CMP kinase	9888	R4_1416	100.00	6E-23	56
Danio rerio	NP_998350	-	2332	R4_661r	100.00	3E-23	57
Danio rerio	NP_998361	polypeptide N-acetylgalactosaminyltransferase 6	1185	R4_1168	100.00	4E-22	55

Annex 2

Danio rerio	NP_998479	NEDD8-conjugating enzyme UBE2F	13661	R4_14767	100.00	9E-22	54
Danio rerio	NP_998529	-	351	R4_37198r	100.00	5E-22	55
Danio rerio	NP_998547	splicing factor, arginine/serine-rich 2	8318	R4_218r	100.00	5E-22	55
Danio rerio	NP_998548	-	1834	R4_1775	100.00	2E-22	55
Danio rerio	NP_998552	phosphoglycerate kinase 1	3502	R4_18103	100.00	3E-22	55
Danio rerio	NP_998651	ubiquitin-conjugating enzyme E2Na	420	R4_9995	100.00	5E-22	55
Danio rerio	NP_999856	-	4262	R4_21887r	100.00	4E-22	55
Danio rerio	NP_999869	cytosolic non-specific dipeptidase	845	R4_872	100.00	3E-22	55
Danio rerio	NP_999924	-	248	R4_307	100.00	3E-22	55
Danio rerio	NP_999947	DNA primase large subunit	4765	R4_4664r	98.18	4E-20	55
Danio rerio	NP_999975	carboxypeptidase E precursor	934	R4_51605.2	100.00	4E-22	55
Danio rerio	NP_999985	adenylosuccinate synthetase isozyme 1	11340	R4_12406	100.00	2E-22	55
Danio rerio	XP_001922856	-	54594	R4_36650.2	100.00	7E-23	55
Danio rerio	XP_001923886	PREDICTED: microtubule-associated protein RP/EB family member 3-like isoformX1	40161	R4_24827r	100.00	2E-22	55
Danio rerio	XP_002661386	PREDICTED: nicotinamide phosphoribosyltransferase-like	23855	R4_33061r.1	98.18	2E-20	55
Danio rerio	XP_002662361	PREDICTED: nodal modulator 2	39676	R4_24482	100.00	1E-22	55
Danio rerio	XP_002662564	-	39836	R4_24592	100.00	2E-21	53
Danio rerio	XP_002664258	-	14015	R4_15137	100.00	1E-22	55
Danio rerio	XP_002664493	-	86108	R4_8269	100.00	2E-22	55
Danio rerio	XP_002666146	-	9551	R4_10732	100.00	4E-22	55
Danio rerio	XP_002667793	-	41295	R4_25707r	100.00	1E-22	55
Danio rerio	XP_002667797	PREDICTED: troponin I, slow skeletal muscle-like	2820	R4_2724	100.00	2E-22	55
Danio rerio	XP_003198647	PREDICTED: proline dehydrogenase, mitochondrial-like	2349	R4_2260	100.00	2E-22	55
Danio rerio	XP_003200317	-	87221	R4_64040r	100.00	8E-23	55
Danio rerio	XP_003200733	PREDICTED: inosine triphosphate pyrophosphatase-like	35029	R4_1302	100.00	4E-23	56

Annex 2

Danio rerio	XP_683819	PREDICTED: phosphatidylinositol 3-kinase regulatory subunit alpha isoformX1	14240	R4_15391r	100.00	1E-22	56
Dicentrarchus labrax	CBN80589	-	5407	R4_5339	100.00	2E-22	55
Dicentrarchus labrax	CBN81647	Collagen type I alpha 3 chain	3	R4_14936	100.00	6E-23	56
Heterocephalus glaber	S61A1_DANRE	deltex-3-like protein	1860	R4_15782	100.00	4E-22	55
Ictalurus furcatus	ADO28411	myosin regulatory light polypeptide 9	484	R4_567	100.00	4E-22	55
Ictalurus punctatus	NP_001187492	GTP-binding protein SAR1b	702	R4_69353r	100.00	1E-22	56
Ictalurus punctatus	NP_001187506	proteasome subunit alpha type-2	601	R4_658.1	100.00	3E-22	55
Ictalurus punctatus	NP_001187576	DNA-directed RNA polymerases i II and III subunit rpabc3	3171	R4_3056r	100.00	2E-22	55
Ictalurus punctatus	NP_001188051	-	15734	R4_17075	100.00	3E-22	55
Makaira nigricans	AAB58117	ryanodine receptor RyR1 isoform	51525	R4_34029	100.00	7E-23	55
Monodelphis domestica	XP_001367631	PREDICTED: ryanodine receptor 1-like	4756	R4_4655.2	100.00	5E-22	55
Oreochromis niloticus	XP_003438811	PREDICTED: protein kinase C and casein kinase substrate in neurons protein 2-like	16730	R4_8220	100.00	3E-22	55
Oreochromis niloticus	XP_003440056	-	24730	R4_44694r	98.18	2E-20	55
Oreochromis niloticus	XP_003441220	-	14123	R4_3720	100.00	1E-22	55
Oreochromis niloticus	XP_003441728	-	74189	R4_52684	100.00	2E-22	55
Oreochromis niloticus	XP_003444566	PREDICTED: natterin-4-like	12259	R4_13322	100.00	2E-22	55
Oreochromis niloticus	XP_003445129	-	38872	R4_23855r.1	100.00	2E-22	55
Oreochromis niloticus	XP_003446273	PREDICTED: gap junction beta-3 protein-like	1056	R4_1055.1	100.00	4E-22	55
Oreochromis niloticus	XP_003447126	PREDICTED: cat eye syndrome critical region protein 5 homolog	45413	R4_28974	100.00	8E-23	55
Oreochromis niloticus	XP_003447427	PREDICTED: neurabin-1-like isoform X1	2525	R4_5993	100.00	3E-22	55
Oreochromis niloticus	XP_003450550	PREDICTED: nuclear inhibitor of protein phosphatase 1-like isoform X1	45196	R4_7144	100.00	2E-22	55
Oreochromis niloticus	XP_003451348	PREDICTED: UDP-N-acetylglucosamine transporter-like isoform X1	19082	R4_30568r	98.18	3E-20	55

Annex 2

Oreochromis niloticus	XP_003455198	PREDICTED: transmembrane emp24 domain-containing protein 2-like isoform X1	6954	R4_52037r	100.00	5E-22	55
Oreochromis niloticus	XP_003456387	-	36510	R4_10814	100.00	2E-22	55
Salmo salar	ACM09792	C14orf166	2598	R4_2508	100.00	2E-22	55
Salmo salar	NP_001133614	EH domain-containing protein 3	1589	R4_1536	100.00	1E-22	56
Scophthalmus maximus	ABJ98621	interferon-inducible protein Gig1, partial	205	R4_235.2	100.00	2E-23	57

7.3. Annex 3

The list of brill DE genes is provided in digital format as an excel file, and contains central trend and dispersion statistical measures and associated t-test p-value.

7.4. Annex 4

The list of turbot DE genes is provided in digital format as an excel file, and contains central trend and dispersion statistical measures and associated t-test p-value.

7.5. Annex 5

The list of between species DE genes is provided in digital format as an excel file, and contains associated t-test p-value.

7.6. Annex 6

Annex 6. Functional categories associated to the represented genes in the Tables 3-8 (62 genes).

Brill up-regulated functions (p < 0,2)												
Category	**Term**	**Count**	**%**	**P Value**	**Genes**	**List Total**	**Pop Hits**	**Pop Total**	**Fold Enrichment**	**Bonferroni**	**Benjamini**	**FDR**
KEGG_PATHWAY	ptr04115:p53 signaling pathway	2,00	1,67	0,07	CDK1, SERPINE1	6,00	67,00	4407,00	21,93	0,75	0,75	43,16
KEGG_PATHWAY	ptr04110:Cell cycle	2,00	1,67	0,13	CDK1, MCM4	6,00	117,00	4407,00	12,56	0,91	0,70	62,92
Brill down-regulated functions (p < 0,1)												
Category	**Term**	**Count**	**%**	**P Value**	**Genes**	**List Total**	**Pop Hits**	**Pop Total**	**Fold Enrichment**	**Bonferroni**	**Benjamini**	**FDR**
GOTERM_BP_FAT	GO:0048514~blood vessel morphogenesis	2,00	2,86	0,03	VEGFA, TNNI3	2,00	21,00	734,00	34,95	0,63	0,63	22,53
GOTERM_BP_FAT	GO:0001568~blood vessel development	2,00	2,86	0,03	VEGFA, TNNI3	2,00	24,00	734,00	30,58	0,68	0,43	25,35
GOTERM_BP_FAT	GO:0001944~vasculature development	2,00	2,86	0,03	VEGFA, TNNI3	2,00	25,00	734,00	29,36	0,69	0,32	26,27
Turbot up-regulated functions (p < 0,1)												
Category	**Term**	**Count**	**%**	**P Value**	**Genes**	**List Total**	**Pop Hits**	**Pop Total**	**Fold Enrichment**	**Bonferroni**	**Benjamini**	**FDR**
GOTERM_BP_FAT	GO:0006259~DNA metabolic process	3,00	2,70	0,03	TNFRSF6B, FOS, RAD9A, RTEL1	9,00	506,00	13528,00	8,91	1,00	1,00	34,85
GOTERM_BP_FAT	GO:0033554~cellular response to stress	3,00	2,70	0,04	TNFRSF6B, FOS, RAD9A, RTEL1	9,00	566,00	13528,00	7,97	1,00	0,98	41,07
GOTERM_BP_FAT	GO:0000302~response to reactive oxygen species	2,00	1,80	0,04	FOS, SERPINE1	9,00	75,00	13528,00	40,08	1,00	0,95	42,69
GOTERM_BP_FAT	GO:0007568~aging	2,00	1,80	0,06	FOS, SERPINE1	9,00	110,00	13528,00	27,33	1,00	0,96	55,85
GOTERM_BP_FAT	GO:0051052~regulation of DNA metabolic process	2,00	1,80	0,07	TNFRSF6B, RAD9A, RTEL1	9,00	114,00	13528,00	26,37	1,00	0,93	57,15
GOTERM_BP_FAT	GO:0006979~response to oxidative stress	2,00	1,80	0,09	FOS, SERPINE1	9,00	164,00	13528,00	18,33	1,00	0,96	70,52
Turbot down-regulated functions (p < 0,1)												
Category	**Term**	**Count**	**%**	**P Value**	**Genes**	**List Total**	**Pop Hits**	**Pop Total**	**Fold Enrichment**	**Bonferroni**	**Benjamini**	**FDR**
GOTERM_BP_FAT	GO:0001501~skeletal system development	3,00	1,29	0,01	MGP, COL5A2, PRELP	6,00	319,00	13528,00	21,20	0,26	0,26	5,12
GOTERM_BP_FAT	GO:0030199~collagen fibril organization	2,00	0,86	0,01	COL5A2, DPT	6,00	29,00	13528,00	155,49	0,46	0,26	10,09

Annex 6

GOTERM_BP_FAT	GO:0030198~extracellular matrix organization	2,00	0,86	0,04	COL5A2, DPT	6,00	104,00	13528,00	43,36	0,89	0,52	31,79
GOTERM_BP_FAT	GO:0001503~ossification	2,00	0,86	0,04	MGP, COL5A2	6,00	115,00	13528,00	39,21	0,91	0,46	34,50
GOTERM_BP_FAT	GO:0060348~bone development	2,00	0,86	0,04	MGP, COL5A2	6,00	123,00	13528,00	36,66	0,93	0,41	36,41
GOTERM_BP_FAT	GO:0043062~extracellular structure organization	2,00	0,86	0,06	COL5A2, DPT	6,00	163,00	13528,00	27,66	0,97	0,44	45,17
Between species diverged functions (p < 0,05)												
Category	**Term**	**Count**	**%**	**P Value**	**Genes**	**List Total**	**Pop Hits**	**Pop Total**	**Fold Enrichment**	**Bonferroni**	**Benjamini**	**FDR**
GOTERM_BP_FAT	GO:0048661~positive regulation of smooth muscle cell proliferation	2,00	1,11	0,02	VEGFA, HBEGF	15,00	15,00	13588,00	120,78	0,99	0,99	18,62
GOTERM_BP_FAT	GO:0042127~regulation of cell proliferation	4,00	2,22	0,02	VEGFA, HBEGF, CDCA7L, DPT	15,00	538,00	13588,00	6,74	0,99	0,91	19,56
GOTERM_BP_FAT	GO:0048660~regulation of smooth muscle cell proliferation	2,00	1,11	0,02	VEGFA, HBEGF	15,00	20,00	13588,00	90,59	1,00	0,87	24,02
GOTERM_BP_FAT	GO:0030199~collagen fibril organization	2,00	1,11	0,02	COL5A2, DPT	15,00	21,00	13588,00	86,27	1,00	0,80	25,06
GOTERM_BP_FAT	GO:0000278~mitotic cell cycle	3,00	1,67	0,03	CDK1, GM11223, STMN1, STMN1-RS2, AURKB	15,00	244,00	13588,00	11,14	1,00	0,78	28,96
GOTERM_BP_FAT	GO:0051301~cell division	3,00	1,67	0,03	CDK1, AURKB, TOP2A	15,00	281,00	13588,00	9,67	1,00	0,80	35,96
GOTERM_BP_FAT	GO:0000279~M phase	3,00	1,67	0,03	CDK1, GM11223, STMN1, STMN1-RS2, AURKB	15,00	283,00	13588,00	9,60	1,00	0,76	36,34
GOTERM_BP_FAT	GO:0008284~positive regulation of cell proliferation	3,00	1,67	0,03	VEGFA, HBEGF, CDCA7L	15,00	284,00	13588,00	9,57	1,00	0,71	36,53
GOTERM_BP_FAT	GO:0051272~positive regulation of cell motion	2,00	1,11	0,04	GM11223, HBEGF, STMN1, STMN1-RS2	15,00	41,00	13588,00	44,19	1,00	0,75	43,08
GOTERM_BP_FAT	GO:0022403~cell cycle phase	3,00	1,67	0,04	CDK1, GM11223, STMN1, STMN1-RS2, AURKB	15,00	328,00	13588,00	8,29	1,00	0,73	44,81